SISSA - SCUOLA
INTERNAZIONALE
SUPERIORE
DI STUDI AVANZATI
TRIESTE
Strada Costiera 11

ISAS - INTERNATIONAL SCHOOL FOR ADVANCED STUDIES

THESIS FOR THE TITLE OF

"MAGISTER PHILOSOPHIAE"

SPECTROPHOTOMETRIC MODELS OF GALAXIES

Section: Astrophysics

Supervisor: Prof. G. Barbaro

Candidate: Fabrizio Olivi

Academic Year: 1985/86

TRIESTE

INDEX.

1. INTRODUCTION 1

2. FORMULATION OF THE MODEL 2

3. THE STELLAR BIRTH-RATE C(m,t) 5

3.1 Initial mass function (IMF) 5

3.2 Rate of star formation 11

4. INPUT FROM THE THEORY OF THE STELLAR STRUCTURE 12

4.1 Main sequence stars (MS) 14

4.2 Red giant branch stars (RGB) 15

4.3 He-burning 16

4.4 Asymptotic giant branch stars (AGB) 19

4.4.1 Synthetic AGB evolutionary models 19

4.4.2 Effects of overshooting on AGB stars 23

4.5 The critical masses M_{HeF}, M_{w}, M_{up} and M_{mas} 24

4.6 Evolutionary background used in the model 25

5. INPUT FROM THE THEORY OF STELLAR ATMOSPHERES 26

6. COSMOLOGICAL APPLICATIONS OF THE MODEL 31

6.1 The apparent magnitude redshift diagram (m - z) 32

6.2 The count-apparent magnitude diagram (N_m - m) 34

7. THE SPECTRA OF THE STELLAR GENERATIONS 38

7.1 Young stellar generations 38

7.2 The spectra of old stellar generations 44

7.2.1 Integrated spectra with $Z=10^{-2}$ 44

7.2.2 Integrated spectra with $Z=10^{-4}$ 46

8. SPECTRAL EVOLUTION OF GALAXIES 52

8.1 Galactic synthetic spectral energy distributions 52

8.2 Galaxy synthetic spectral evolution 57

8.3 Observational test for galaxy evolution 58

8.3.1 Broad-band galaxy counts 58

8.3.2 Broad band photometric comparisons 59

8.3.3 Spectrophotometric comparisons 59

1. INTRODUCTION.

The purpose of this thesis is to discuss critically the possibility of synthesizing the integrated spectrum of normal galaxies and to describe its evolution.

The need for such models is twofold: first to decode informations contained in the integrated light of galaxies in order to define their stellar populations; second, provided that the first goal is reached, to predict the integrated spectral energy distribution (SED) of galaxies seen at large "look-back" time (at high redshift).

The necessity for using integrated properties in the study of galaxies arises because, with the exception of nearest ones, the galaxies cannot be resolved in single stars. Although the problem has been faced since nearly half a century ago (Wipple 1935), only in the last two decades have two efficient techniques been developed to cast light on the populations of unresolved galaxies: the population synthesis and the evolutionary synthesis. We shall use the second method, by which the integrated light of a galaxy can be modelled by making suitable assumptions on the stellar birth rate and following the evolution of its population: in this way it is possible not only to derive the population and the SED at the present time but also their past evolution can be reconstructed.

Moreover from the comparison of the observed spectrum of a nearby galaxy with a set of model spectra an estimate of the age of a galaxy can be derived. In principle, the extending of this

procedure to a great number of galaxies, at greater and greater redshifts, should allow a direct evaluation of the look-back time as a function of the redshift, independently of the cosmological time, therefore improving the determination of the fundamental cosmological quantities H_0 e q_0.

2. FORMULATION OF THE MODEL.

At least in principle one cannot enucleate the problem of the population and spectral evolution from the general evolutionary frame and particularly one cannot neglect dynamic and chemical evolution. The present knowledge of the star formation theory allows one to foresee how important is the dynamic behaviour of the interstellar medium for the astrogenetic processes and suggests an even more important role during the collapse of the protogalaxies. On the other hand the importance of the chemical evolution is evident as it defines one of the basic parameters characterizing the stellar populations: the metal content.

Although Larson and Tinsley (1974) followed simultaneously the dynamic, chemical and photometric evolution of a galaxy model, still the inclusion of the dynamic factors in the integrated light synthesis at present requires considerable effort which is not rewarded by proportionate advantages, since the present status of the theory of star formation is unable to correlate the star formation rate to the state of the interstellar medium. The chemical evolution, on the contrary, can

be computed without particular difficulties, at least in an approximate form, to derive the time dependence of the metal content of the interstellar gas and therefore the initial chemical composition of each generation of stars which enters in the model synthesis. The distinction between populations of different chemical composition is important in general but seems to be fundamental in models whose light is dominated by old stars since, from the theory of stellar evolution it is well known that the metal content strongly affects the lifetime and effective temperature during some evolutionary phases.

The synthetic approach is generally based on the following simplifications:

- the non-thermal emission from the interstellar gas is negligible; this automatically rules out the possibility of modelling active galaxies, whose activity cannot be ascribed to the stars;
- the thermal emission from the interstellar gas is negligible; Huchra (1977) in fact has shown that the continuum emission from the interstellar gas is negligible compared to that of stars;
- the absorption of light from gas and dust can be neglected. Although this approximation is fairly correct for the models of early type galaxies, it does not seem justified in the case of late-type galaxies, where gas and dust are present in considerable amount.

Therefore, on these grounds, the integrated light of a galaxy is the superimposition of the light emitted from all the stars that populate the system.

Let $f_\lambda(m,\tau,Z)$ denote respectively the monochromatic flux emitted by a star of mass m, age τ and metal content Z, and C(m,t) the stellar birth-rate; the integrated monochromatic flux of the galaxy is given by:

$$F_\lambda(T) = \int_0^T \int_{m_L}^{m_U} C(m,t)\ f_\lambda(m,\tau,Z)\ dt\ dm \qquad (1)$$

with $\tau = T - t$

where T is the age of galaxy and (m_L, m_U) the stellar mass interval.

In principle the evaluation of F_λ requires the contribution of several theories:

a) The star formation theory which should supply us with the stellar birth rate C(m,t); however, as already remarked, the present status of development of this theory does not allow the derivation of reliable estimates for the birth rate in terms of physical conditions of the interstellar gas.

b) Theory of chemical evolution which yields the function Z(t) describing the evolution of the metal content.

c) Theory of stellar evolution by which the luminosity and effective temperature of the stars are evaluated as functions of the mass, chemical composition and age. Some difficulties can arise due to the uncertainties connected with the treatment of advanced phases, whose contribution cannot be neglected without affecting the model and to the lack of a sufficient number of evolutionary computations.

d) Theory of stellar atmosphere from which we derive the stellar

SED f_λ in terms of effective temperature, surface gravity and chemical composition.

3. THE STELLAR BIRTH-RATE C(m,t).

As already remarked, the present status of development of the star formation theory does not allow the theoretical derivation of reliable estimates for the birth-rate; so one is compelled to make reasonable hypothesis.

In general the assumption is made that the function C(m,t) can be expressed as the product of two functions: the one of the stellar mass the other of the age of the system

$$C(m,t) = \phi(m) \cdot B(t).$$

For a fixed t $\phi(m)$ gives the mass distribution of a single generation of stars; this function is named "initial mass function" (IMF), and is normalized with the condition:

$$\int_{m_L}^{m_U} \phi(m)\, dm = 1 \quad .$$

Moreover from

$$\int_{m_L}^{m_U} C(m,t)\, dm\, dt = B(t)\, dt \int_{m_L}^{m_U} \phi(m)\, dm = B(t)\, dt$$

it turns out that B(t) is the number of stars formed at the time t per unit time, B(t) is called "rate of star formation" (SFR).

3.1 Initial mass function (IMF).

This function is obtained from observation of samples of

stars (field stars, members of young open clusters and OB association). The procedure is the following:

a) From the observed magnitude M_V and colour index $(B - V)_O$ an estimate of the mass is derived by one of the two methods: 1) use of the empirical mass - luminosity relation, 2) use of evolutionary paths in the HR diagram and comparison with the location of the stars in this diagram: this comparison requires the employment of bolometric correction and colour-temperature relations.

Both method are affected by uncertainties connected with the observations and the theoretical back ground. To reduce the error sources, the consideration is limited to those classes of stars, the evolution of which has been completed with a sufficient accuracy. In fact most of the authors who have dealt with this problem have taken into account only Main Sequence stars. In some cases also massive stars in later phases (for instance red supergiants, WR stars) have been considered; particular care has been used in the choice of the corresponding evolutionary tracks (Garmany et al. 1982, Bisiacchi et al. 1982).

b) From the derived masses a distribution function $\psi(m)$ is obtained for all the sample stars. This function does not coincide with the IMF $\phi(m)$ since the sample generally includes several generations of stars with different ages. Therefore a relation must be derived between the two functions.

Let us suppose that the sample consists of field stars and denote with B(t) the rate of star formation. The number of stars of a given mass which are now present in the sample is the

difference between the number of the stars born and the number of stars which are dead during the lifetime of the system. This implies the subdivision of the stars into two group according to their mass: 1) Stars with $m < m_o$ where m_o is the mass whose lifetime $t_{lf}(m)$ is equal to the age T of the system. The lifetime of these stars is larger than T and therefore none of them is already dead. 2) Stars with $m > m_o$, whose lifetime is smaller than T.

Therefore the number of stars per unit mass with $m_i < m_o$ which are present in the sample is

$$\psi(m)\ dm = \phi(m)\ dm \int_0^T B(t)\ dt \qquad (m_i \leq m_0).$$

The number of stars per unit mass with $m_i > m_0$ is give by:

$$\psi(m)\ dm = \phi(m)\ dm \int_0^T B(t)\ dt - \phi(m)\ dm \int_0^{T-t_{lf}(m)} B(t)\ dt$$

where the second term at the second member gives the number of dead stars.

$$\psi(m)\ dm = \phi(m)\ dm \int_{T-t_{lf}(m)}^T B(t)\ dt \qquad (m_i > m_0).$$

Therefore the relation between $\psi(m)$ and $\phi(m)$ is not univocally determined, since it requires the definition of B(t). The determination of the rate of star formation over all the history of the sample is very difficult, although some constraints can be put a posteriori by the behaviour of the obtained $\phi(m)$ at low masses. In fact Miller and Scalo (1979) have shown that the initial mass function $\phi(m)$ derived by imposing a rate of star formation quickly decreasing with the time, exhibit a

discontinuity at $m = m_o$; as there is no physical reason for the existence of such a discontinuity, rates of star formation with a small time scale are to be excluded. In fact there are indications that in the solar neighbourhood the past stellar birth rate has not sensibly changed over the past 5 billion years.

In deriving the IMF usually the assumption is made that B(t) is constant.

When the sample is formed by the stars of an open clusters $\psi(m)$ and $\phi(m)$ coincide, since it is generally believed that the cluster stars are contemporary and constitute a single generation.

When the sample is made of field stars, one must remember that the distribution of the disk stars in the direction perpendicular of the galactic plane it is a function of their absolute magnitude the most luminous being more concentrated towards the galactic plane. In fact if $\rho_{Mv}(r,\theta,z)$ denotes the number of stars per unit volume with absolute magnitude M_v it turns out from observations that:

$$\rho_{Mv}(r,\theta,z) = \rho_{Mv}(r,\theta|0)\, e^{-(|z|/H(Mv))}$$

where the half thickness H is a function of M_v as is shown in Table I (Miller and Scalo 1979).

Table I

M_v	2H (pc)
-6	180
-5	180
-4	180
-3	180
-2	180
-1	180
0	180
+1	185
+2	210
+3	300
+4	465
+5	590
+6	635
+7	650
+8	650
+9	650
+10	650
+11	650
+12	650
+13	650
+14	650
+15	650
+16	650

The reason for such a behaviour are not clear, however it seems to depend on dynamic mechanism; anyhow this effect must be removed in deriving the IMF. This can be reached by using the column densities. The column density σ and the volume density are easily correlated:

$$\sigma_{Mv}(r,\theta) = \rho_{Mv}(r,\theta|0) \int_{-\infty}^{+\infty} e^{-(|z|/H(Mv))} dz = 2\, H(Mv)\, \rho_{Mv}(r,\theta|0).$$

Among the several determinations of the IMF the majority are in the form:

$$\log \phi(m) = A - \alpha \log m$$

Where A and α are constant. In some cases a better fit of the data is obtained with different values of α in different mass ranges.

After the first work of Salpeter (1955) who derived for α

the value of 2.35, several papers have been devoted to this subject.

Salpeter's value of α is still accepted in the mass range (1 - 10) $M_\odot$.

In the higher mass range (10 - 100) $M_\odot$ Lequeux (1979) and Miller and Scalo (1979) derived a larger value: $\alpha \simeq 3$, afterwards the use of more recent evolutionary tracks lowered again this value to 2.5 (Garmany at al. 1982).

In the lower mass range the value estimated is fairly low (α = 1.4 Miller and Scalo 1979). Current evidence does not supports the existence of a large number of low-mass stars; in fact recent data indicate that the mass function peaks at a mass near 0.25 $M_\odot$ and drops steeply at lower masses (Larson 1986).

On these grounds the IMF should not be a monotonic function of the stellar mass but a double-peaked function; Larson (1986) adopted the following IMF:

$$C(m,t) = C_1(m,t) + C_2(m,t)$$

where $$C_i(m,t) = B_i(t)\ \phi_i(m,t)$$

$$\phi_i(m)\ dm = A\ m_i\ m^{-3}\ \exp[-(m_i/m)^{3/2}]$$

with $$m_1 = 0.30\ M_\odot \quad \text{and} \quad m_2 = 2.2\ M_\odot$$

This function approximates a power law at large masses while at low masses shows an exponential cut off for $m < 0.25\ M_\odot$.

The shape of IMF has been investigated also by a theoretical approach based on the hypothesis of a fragmentation due to gravitational instability (Di Fazio and Capuzzo-Dolcetta 1986), the bimodal behaviour is confirmed.

An universal IMF is excluded by recent studies indicating a

variation of IMF with the metal content; in particular the following relationship between the slope α of the IMF and the metal content of the interstellar medium Z is suggested:

$$\alpha = \log Z + 5.05$$

for a mass range (0.1 - 100 $M_{\odot}$) (Matteucci and Tornambe' 1985).

3.2 Rate of star formation.

The rate of star formation (SFR) B(t) gives at a given instant t the number of the star born in the unit time, whatever their mass can be.

Although the theories on the interstellar medium and star formation (SF) are not capable of deriving suitable expressions for the SFR, still they suggest that the star formation is rather a complex process and depends on several parameters, the most important of them being the local density of molecular gas. Several attempts have been made in order to correlate the SFR to the gas density. Estimates for the SFR can be derived by counts of young objects like OB stars, HII regions, supernova remnant, cepheids, etc. The density of the H can be obtained from the flux of the line at 21 cm. for neutral atomic H, and from the emission of CO in the case of molecular H.

The first attempt in this sense has been done by Schmidt (1959) who fitted the observations in the solar neighbourhood with a relation $B \propto \rho_G^{\,n}$ and found for n the value of 2. Afterwards several other papers have been devoted to this task yielding sometimes rather different results.

Talbot (1980) investigated this relation by assuming the rate of formation of massive stars to be proportional to the emission per unit area from the ionized hydrogen. He then plotted this quantity against the surface density of total gas (ρ_G), atomic hydrogen (ρ_{HI}) and molecular hydrogen (ρ_{H_2}) and concluded that the rate of formation of massive stars is more significantly correlated with ρ_{H_2} than with ρ_{HI} or ρ_G. Table II shows his estimate of n and the correlation coefficient R_c. These results have been confirmed by a recent work of Rana and Wilkinson (1986).

Table II

density type	n	R_c
ρ_{HI}	-4.3 ± 0.7	-0.86
ρ_{H_2}	0.94 ± 0.19	0.79
ρ_G	1.49 ± 0.37	0.37

In our models we shall use both a SFR derived from dynamical models or expressed by a simple analytical formula with one or more parameters. The more used parametrisation for B(t) is:

$$B(t) = A\ \beta\ e^{-\beta t}$$

the value of β is in the range 0-10 when t is expressed in units of 10^{10} yr.

If a bimodal SF is assumed, B(t) has a different behaviour for low and high masses; Larson (1986) uses for our Galaxy a constant SFR for low mass star and a decreasing one with β=2.9 for stars of larger mass.

4. INPUT FROM THE THEORY OF THE STELLAR STRUCTURE

The evolution of the stars strongly depends on their initial

mass. So we shall use classify them according to their initial mass (Chiosi 1986):

1) Massive stars ($m_i > M_{mas}$): These stars proceed through a series of nuclear burnings in non degenerate conditions towards the construction of an iron core, subsequent instability due to the photodissociation, core collapse and supernova explosion. The classical value of M_{mas} is 12 $M_\odot$.

2) Quasi-massive stars ($M_{up} < m_i < M_{mas}$): stars in this mass range ignite carbon non violently. Their subsequent evolution is very complicated and eventually ends with a supernova explosion (Nomoto 1984). The classical value of M_{up} is $9M_\odot$ for the chemical composition of Pop I stars and $M_{up} = 7M_\odot$ for Pop II (Becker and Iben 1979).

3) Intermediate mass stars ($M_{HeF} < m_i < M_{up}$): stars in this mass range ignite He non degenerately but following He-exhaustion in the core develop a highly degenerate CO core. They evolve across the AGB phase, during which they undergo a series of thermal pulses and their evolution is terminated either by envelope ejection and formation of a white dwarf (for $M_{HeF} < m_i < M_w$) or carbon by ignition and deflagration in a highly degenerate core which has grown up to the Chandraseckar limit (1.4 $M_\odot$). This event is usually referred to as supernova of type I1/2 (Iben and Renzini 1983). The classical value of M_w is 5 $M_\odot$ (Iben and Renzini 1983). The limit M_{HeF} has the value 2.2 $M_\odot$ Pop. I and 1.8 M_O for Pop. II.

4) Low mass stars ($m_i < M_{HeF}$): these stars develop a highly degenerate He core after the central H exhaustion. They evolve

along the red giant branch, at the tip of which He is ignited violently in the core (He-flash). At this point the core mass has grown up to about 0.5 $M_\odot$, depending on the chemical composition. Their subsequent evolution is quite similar to that of intermediate mass stars. The classic value of M_{He} is 2.2 to 2.3 $M_\odot$ for Pop I and about 1.8 $M_\odot$ for Pop II chemical composition.

Evolutionary models have been recently modified by the introduction of two physical processes strongly affecting the evolution: mass loss and overshooting. The inclusion of those processes has improved the agreement with the observational data.

4.1 Main sequence stars (MS).

Mass loss during the main sequence is important only for massive stars; the following effects arise when mass loss is accounted for:

1) The mass of the convective core decreases more rapidly.
2) The MS lifetime is somewhat increased.
3) For moderate mass loss, there is a slight MS widening.
4) The mass of the He core at the end of the core H-burning is smaller.

Overshooting concerns only those stars which develop a convective core and therefore is limited to the stars with $m_i > M_{LC} = 1.2\ M_\odot$ (Bertelli et al. 1985). Generally the border of the convective core is defined by the equality condition of the radiative and adiabatic gradients; the boundary is put therefore where the forces acting on the convective elements vanish, in

this way one neglects the fact that the convective elements overshoot this boundary, due to the non vanishing velocity they have at the boundary itself.

To account for this overshoot has the following consequences on the evolution during the MS phase:

1) The mass of convective core is significantly greater.

2) Stars evolve toward higher luminosity.

3) The MS lifetime is increased.

4) The MS band in the HR diagram is much wider.

In this way the agreement between theoretical and observed location on the HR diagram are significantly improved (Bertelli et al. 1984).

4.2 Red giant branch stars (RGB).

The RGB is populated by stars which, following the core H exhaustion, during the shell H burning develop a degenerate core. The inclusion of the overshooting during the MS phase raises the mass of the He core at the beginning of the H shell burning.

During the ascent along the RGB stars lose a larger fraction of their envelops.

Evolutionary computations show that the behaviour of the red giants is essentially not affected by the this mass loss, which on the contrary significantly influences the following phases (Fusi Pecci and Renzini 1975).

The overluminosity caused by the overshooting during core H-burning phase still remains during the shell H phase (Bertelli et

al. 1985).

During this phase a larger convective zone deepens from the outer layer into the star. Since outer convection cannot be considered with reliability as adiabatic, it must be treated according to the mixing length theory. Due to the roughness of this theory the position of the models in the HR diagram is rather uncertain and this can influence synthetic spectra.

4.3 HE-burning.

The He-burning phases of massive stars are sensibly influenced by the mass loss. It causes an apparently erratic location in the HR diagram. Indeed, this location is extremely sensitive to many structural properties.

In very massive stars the wind responsible for mass loss during the main sequence and early shell H-burning is high enough to remove all the outer layers, leaving a bare He core. This prevents evolution towards the red supergiant stage, and therefore such stars live their final evolutionary phases on the left half of the HR diagram. This stars are good candidates for the WR stage (Bertelli et al. 1984); so the mass loss also account for single WR stars, not belonging to close binary systems.

For intermediate stars, mass loss is less important and can be neglected while the introduction of the overshooting gives rise to several effects:

1) The star has a higher luminosity.

2) The lifetime of the He-burning phase t_{He} gets shorter as a consequence of the much higher luminosity, the ratio t_{He}/t_H is fairly low; a much higher ratio is given by classic models in the same mass range. This changes completely our expectation for the relative number of post main sequence versus MS stars.
3) Convective overshooting strongly decreases the extension of loops in the HR diagram (Bertelli et al. 1985).

Evolution of low mass stars in this phase correspond to the horizontal branch (HB) phase; their evolution is more uncertain and this can influence the final results of the spectral synthesis because the ultraviolet (UV) flux of an old population strongly depends on the exact position on the HR diagram of horizontal branch stars. The analysis of HR diagram of globular clusters has revealed that the morphology of their HB cannot be interpreted, within the classical evolutionary theory, in terms of change of only one parameter: the metal content. Evidence is growing, on the contrary, that a further parameter is required but its identification is, however, still doubtful. Faced by this difficulties galaxy modelmakers have adopted different solutions: some have simply ignored the He-burning for such stars, others have adopted a semiempirical approach by distributing a suitable number of stars along the zero age HB according to a temperature distribution which depends on one or more parameters and which can be constrained by the observations. Others have adopted the theoretical approach including the effects of mass loss during the shell H-burning which determines the correct mass of stars burning helium. Rood (1973) suggested that the temperature

distribution of the HB stars cannot be interpreted unless the amount of mass lost during the red giant branch changes from star to star giving rise, on the HB, to the following distribution

$$P(m,t) = g(t)\ R(m)$$

$$R(m) = (m - m_c)\ (m_i - m)\ \exp\left[- \left(\frac{m - m_{fl}}{\sigma} \right)^2 \right]$$

where g(t)=const=g and m_{fl} is the most probable value of the mass at the moment of the flash, which can be evaluated from the formulas of Reimers(1975) or of Fusi Pecci and Renzini (1975), m_c is the core mass of the star undergoing the flash; the constant σ has the value 0.025, determined by the fitting with the observed distributions. While the evolutionary approach prevents the modelling of anomalous globular clusters, i.e. clusters whose HB differs from what is expected by the theory for a given metal abundance, it provides the way of computing the HB evolution of a generation of stars, and this indeed is otherwise impossible.

Once determined the position of a star on the zero age horizontal branch we need to know the evolution of this star during the core He-burning phase. Evolutionary models of HB stars are different according to whether overshooting is included or neglected, Bressan et al. (1986) extend the treatment of convective overshooting with a non local description to the range of low mass stars. Their main results can be summarized as follows:

1) The mass of the convective core is greater than that computed under classical conditions.

2) At the end of the core He-burning phase, larger CO cores are built.

3) The lifetime t_{HB} increases.

4.4 Asymptotic giant branch stars (AGB).

During the AGB phase the star moves again near the Hayashi line, therefore the effective temperature T_{eff} is almost constant while the luminosity L changes by some orders of magnitude. Evolution during this phase is very complex since models in the double shell phase are unstable and undergo thermal pulses. To follows the evolution in this phase requires an enormous number of models. This explains the lack of complete works on such an argument and the absence in the literature of sets of evolutionary tracks for this phase. However the evolution on the HR diagram ca be partly constructed with the aid of analytical formulas.

The AGB phase is subdivided into two phases: early AGB (E-AGB) and thermal pulse phase (TP-AGB). The first cannot be reconstructed analytically but can be modelled rather easily (Lattanzio 1986, Becker and Iben 1979). The analytical formulae on the contrary can be derived for second phase, provided that one is not concerned with the loops caused by the thermal pulses.

4.4.1 Synthetic AGB evolutionary models.

The analytical construction proceeds in this way:

1) The starting base is a relation which links the initial mass m_i and the mass below H shell m_H^1 at the start of the first thermal pulse (TP). In general for $m_i < M_{HeF}$ m_H^1 is almost independent of m_i because these stars have ignited the He in the core in degenerate conditions and this occurs only when the core mass approaches a limit value; instead for $m_i > M_{HeF}$ m_H^1 grows with m_i. There are several recipes for this relation:

a) From Lattanzio (1986) for low mass stars ($m_i \leq 3\ M_\odot$)

$$m_H^1 = 0.53 - (1.3 + \log Z)(Y - 0.20) \qquad \text{for POP I}$$

$$m_H^1 = (0.394 + 0.3\ Y)\ e^{(0.10 + 0.3\ Y)\ m_i} \qquad \text{for Pop II } Z = 0.001$$

where m_i and m_H^1 are in solar units.

b) From Iben (1981)

$$m_H^1 = \begin{cases} 0.56 & m_i < 1.35 \\ 0.60 + m_i\ (0.0226\ m_i - 0.0601) & 1.35 < m_i < 4.7 \\ 0.535 + 0.060\ m_i & m_i > 4.7 \end{cases}$$

for Pop I and:

$$m_H^1 = \begin{cases} 0.538 & m_i < 1.0 \\ 0.524 + m_i\ (0.024\ m_i - 0.00988) & 1.0 < m_i < 3.9 \\ 0.654 + 0.0506\ m_i & m_i > 3.9 \end{cases}$$

for Pop II.

c) From Becker and Iben (1979)

$$m_H^1 = \gamma m_i + \delta \qquad \text{with}$$

$$\gamma = 0.0526 + 0.754(Z-Z_0) + 54.4(Z-Z_0)^2 +$$
$$+ 0.222(Y-Y_0) - 1.07(Y-Y_0)^2 + 5.53(Y-Y_0)(Z-Z_0)$$

$$\delta = 5.90 - 10.7(Z-Z_0) - 425(Z-Z_0)^2 +$$
$$- 0.825(Y-Y_0) + 9.22(Y-Y_0)^2 - 44.9(Y-Y_0)(Z-Z_0)$$

2) Once m_H^1 is known it is possible to derive the luminosity at

first TP by means of the following relation:

$$L = 2.925 \times 10^4 \, (m_H - 0.522) \quad \text{(Paczynski 1971)}$$

this formula is derived in the hypothesis that the total L is produced by the H burning shell

$$L \approx L_H$$

this assumption is good enough in the case of low mass stars, for greater masses one cannot neglect the contribution of the gravitational energy, and a more precise relation is:

$$L \approx (L_H + L_{grav}) = 6.36 \times 10^4 \, (m_H - 0.44) \, (m_{TOT}/7)^{0.19}$$

(Iben 1977).

In the low mass range the following relation also can be used:

$$L = (5.925 + 0.415X) \, (m_H - 0.495 + 0.0505X) \, 10^4$$

with $X = [(m_{TOT} - m_H) / 6.04]^{1.83}$ (Iben 1981).

A more complete formulation for low mass stars has been derived by Lattanzio (1986):

$$L = 55350 \, [2.3 \, (Y - 0.20) + 1.0] \, (m_H - a)$$

with $a = 0.489 + 0.23(Y - 0.20) - 0.70(Z - 0.02)$ for Pop I

and $L = 51800[1+4.7(Y-0.20)]m_H - 26260[1+6.2(Y-0.20)]$

for Pop II and Z = 0.001.

3) The effective temperature T_{eff} is related to L by the formula:

$$\log T_{eff} = 3.808 - \gamma \log L + 0.08 \log m$$

with $\gamma = 0.04255 + 0.01 \, (4 + \log Z)$ (Renzini and Voli 1981).

4) The life time of the star during the early-AGB phase can be derived from:

$$\Delta t_{E\text{-}AGB} = \begin{cases} 10^7 \, (2/m_i)^{3.64} & m_i > 2 \, M_\odot \\ 10^7 & m_i < 2 \, M_\odot \end{cases}$$

(Iben and Renzini 1983).

5) At this point the evolutionary path during the TP-AGB phase can be obtained by increasing the luminosity and deriving m_H and T_{eff} according to the previous formulae for each value of L. The evolution along the AGB can end in two ways:

a) the core mass reaches the limiting mass for carbon ignition ($m = 1.4\ M_\odot$); owing to the degenerate conditions in the core the ignition is explosive (supernova type I1/2);

b) before the core mass reaches the limiting value of $1.4\ M_\odot$ the star loses all the envelope entering the phase of planetary nebula and leaving the red part of the HR diagram.

The idea that planetary nebulae are ejected from AGB stars was suggested long before the importance was recognized of stellar winds. The envelope ejection was thought to be caused by a dynamical instability. Observational results seem to suggest that, besides the normal mass loss of cool stars, a more powerful mass loss is required to eject the last envelope layers. This process, called "super wind" starts at a certain L and causes the ejection of envelope in a short time.

Hence the end of the evolution along the AGB is determined by the following tests:

a) comparison of the actual value of m_H with the limiting value for C ignition.

b) evaluation of the envelope mass m_e by determining, by the normal relations for mass loss, the actual mass m of the star, m_e is then given by $m - m_H$. When $m_e = m_{eCRIT}$, where m_{eCRIT} is given by

$$m_{eCRIT} = b\,(1.69 - 8.09 m_H + 11.69 m_H^2 - 4.34 m_H^3)$$

with b a parameter ranging from 1/2 to 1 (Renzini and Voli 1981), the superwind starts and the star becomes a planetary nebula. By means of an iterative process the maximum luminosity is derived.

6) The evolutionary lifetime, starting from the first TP, is derived by:

$$\Delta t = 4.5 \times 10^6 \, \Delta \log L.$$

(Iben and Renzini 1983).

4.4.2 Effects of overshooting on AGB stars.

The introduction of the overshooting in the convective core during the core H and He burning phases gives rise to a different $m_H^1 - m_i$ relation and the mass below the H shell at the first TP changes in this way:

1) for $m_i > 2.2\ M_\odot$ $\quad m_H^{ov} > m_H^c$

2) for $1.6\ M_\odot < m_i < 2.2\ M_\odot$ $\quad m_H^{ov} < m_H^c$

3) for $m_i < 1.6\ M_\odot$ $\quad m_H^{ov} = m_H^c$

(Bertelli et al. 1986), where m_H^{ov} and m_H^c are the values of m_H computed by inclusion of the overshooting and without overshooting respectively.

In the first case, which corresponds to an one non-violent He ignition, the overshooting gives a larger core mass. In the second case which corresponds to a degenerate core configuration and to non-degenerate one depending on whether overshooting is not accounted for or is accounted, m_H^{ov} is shorter than m_H^c because in absence of the degeneracy a smaller core mass is

required for the onset of the burning.

4.5 The critical masses M_{HeF}, M_w, M_{up} and M_{mas}.

The effect of the overshooting on the critical masses is due to the change of core mass:

a) Due to the larger core mass at the beginning of the shell H burning degeneracy is less strong and the flash occurs only if $m_i < 1.6\ M_\odot$.

b) M_{up} is also lowered because of the larger mass of the core; the estimated values are $M_{up} = 6\ M_\odot$ for Z=0.02, Y=0.30 (Pop. I) and $M_{up} = 5\ M_\odot$ for Z=0.001, Y=0.30 (Pop. II).

c) M_{mas} is decreased to 9 $M_\odot$ for Z=0.02, Y=0.30 and to 8 $M_\odot$ for Z=0.001, Y=0.30.

d) The value of M_w depends on the overshooting through the core mass but also on the mass loss. Using the evolutionary tracks of Bertelli et al. (1986), the mass loss formula of Reimers with η = 1/3 and super wind criterion of Renzini and Voli (1981) with b=1, $M_w = 4.03\ M_\odot$ for Z=0.001, Y=0.30 and $M_w = 4.81\ M_\odot$ for Z=0.02, Y=0.30 has been derived.

Table III.

	M_{HeF}	M_w	M_{up}	M_{mas}	Z	Y
no-overshoot	2.2	5	9	12	.02	.3
"	1.8	5	7	12	.001	.3
with-overshoot	1.6	4.81	6	9	.02	.3
"	1.6	4.03	5	8	.001	.3

4.6 Evolutionary background used in the model.

In our model the following evolutionary tracks have been used:

1) For massive stars the tracks of Bressan et al. (1981) with chemical composition Y = 0.30 and Z = 0.02, including overshooting and mass loss.

2) For intermediate mass and quasi massive stars the tracks of Bertelli et al. (1986) with composition Y = 0.30, Z = 0.001 (Fig. 1) and Z = 0.02 (Fig. 2) including overshooting. This tracks stops at the end of E-AGB, so we have constructed the TP-AGB tracks using: a) relation L - m_H from Iben (1977), b) relation T_{eff} - L from Renzini and Voli (1981), d) super wind criterion from Renzini and Voli (1981) with b = 1, e) mass loss according to Reimers with η = 1/3 and e) evolutionary lifetimes from Iben and Renzini (1983).

3) For stars of low mass we have considered three chemical compositions Y = 0.30 and Z = 0.0001, Z = 0.001, Z=0.01. For this range of mass a complete set of tracks with overshooting is not available so we have used a classic scenario with:

i) The isochrones of Ciardullo and Demarque (1977) which include core H and shell H burnings. The temperature of their red giant branches however as been corrected to modify the effect of the mixing length parameter α = 1/Hp which is equal to 1 in the stellar models used by Ciardullo and Demarque. The same authors suggested in fact that the best fit with the observed RGB of old open clusters is reached with α = 1.5. The correction is given

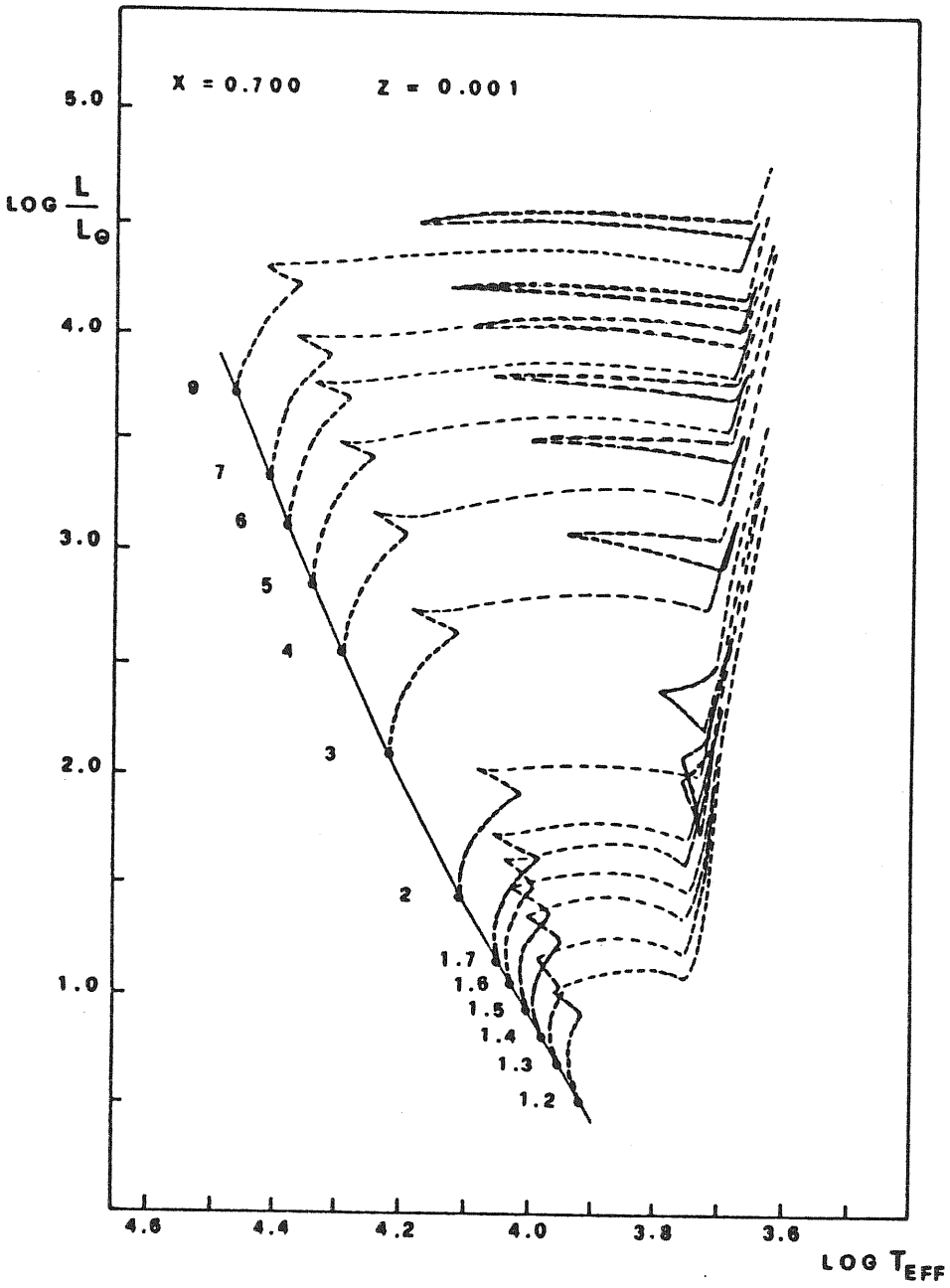

Fig. 1. Evolutionary tracks for intermediate mass and quasi massive stars including overshooting; chemical composition Z=0.001 and Y=0.30 (Bertelli et al. 1986).

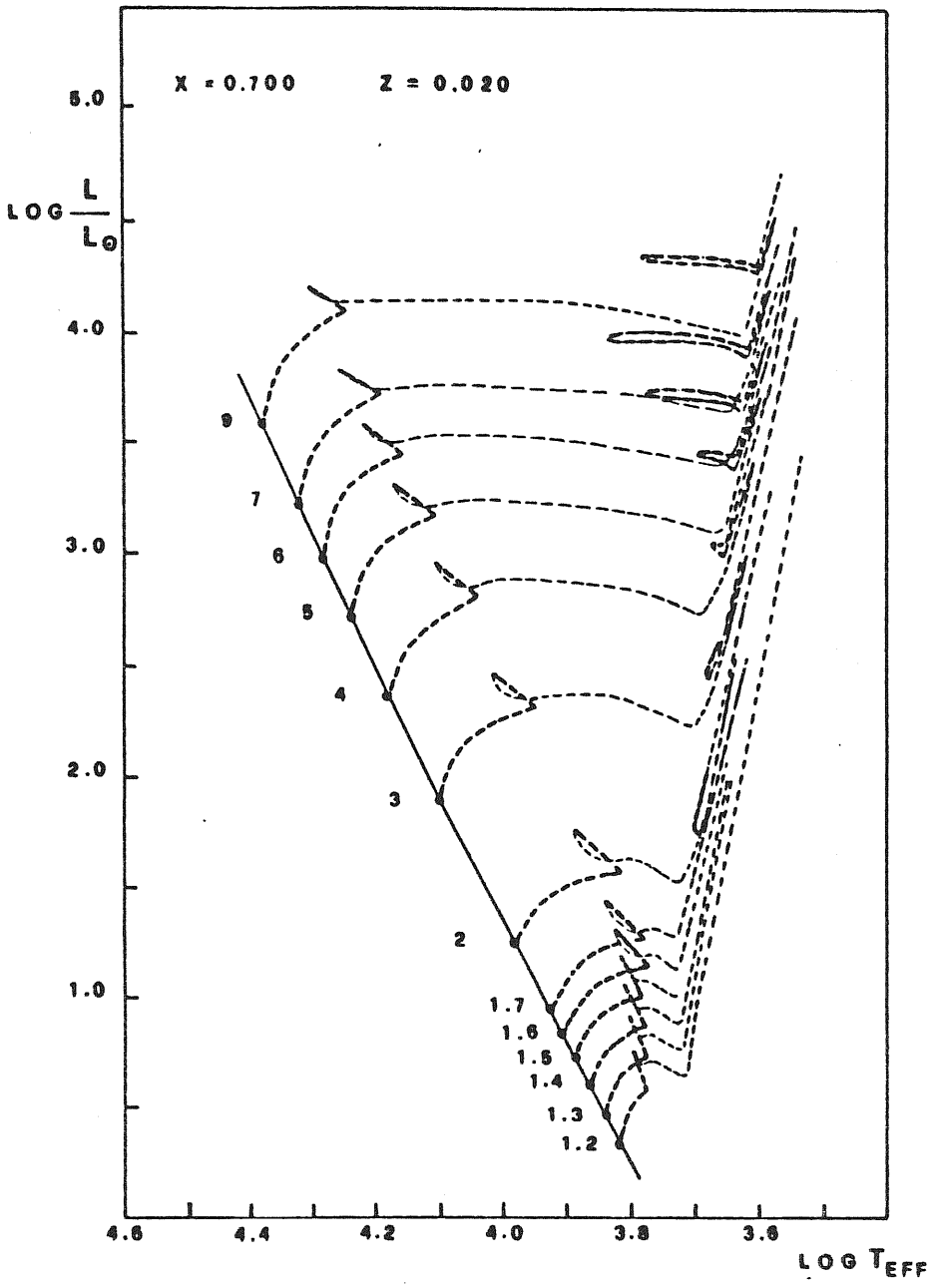

Fig. 2. Evolutionary tracks for intermediate mass and quasi massive stars including overshooting; chemical composition Z=0.02 and Y=0.30 (Bertelli et al. 1986).

by:

$$\log T_{eff} = 0.176\ [0.02\ \log L/L_{\odot} + 0.143]$$

(Ciardullo and Demarque (1979).

ii) For core He-burning the tracks of Sweigart and Gross (1976) have been used. In deriving the isochrones for this phase the actual mass of stars during core He burning has been derived by determining the amount of mass lost during the RGB according to Fusi-Pecci and Renzini (1975). Moreover the mass distribution along the HB has been evaluated according to the relation of Rood (1973).

iii) The AGB phase has been constructed by the following assumptions: a) ($m_i - m_H^1$) and ($L - m_H$) relations from Lattanzio (1986), b) ($T_{eff} - L$) relation and super wind criterion with b=1 from Renzini and Voli (1981), c) mass loss according to Reimers with $\eta = 1/3$ and d) evolutionary lifetimes from Iben and Renzini (1983).

5. INPUT FROM THE THEORY OF STELLAR ATMOSPHERES.

The most adopted and useful models are those of Kurucz (1979) because:

- they cover a wide spectral region: from 229 to 20000 A;
- they have been computed for several values of the metal content ($Z = Z_{\odot}$, $Z = 0.1\ Z_{\odot}$, $Z = 0.01\ Z_{\odot}$);
- the range in effective temperature and surface gravity (g) is wide; for what concerns the temperature the models are computed in the following intervals

$Z = Z_{\odot}$ $\qquad 5500^{o}K \leq T_{eff} \leq 50000^{o}K$

$Z = 0.1\ Z_{\odot},\ Z = 0.01\ Z_{\odot}$ $\qquad 5500^{o}K \leq T_{eff} \leq 10000^{o}K$

The interval of effective temperature and surface gravity covered by the models of Kurucz is however narrower than the whole temperature and gravity range described by the evolutionary tracks and therefore one must make up for this lack. Most reasonable solutions are:

- for low temperatures ($T < 5500^{o}K$) the observed UV and optical spectra of cool stars of the late type can be used;
- for extremely high temperatures ($T > 50000^{o}K$) a good approximation is the black body spectral energy curve because the blanketing effect becomes negligible, all the elements, even the heavier ones, being almost completely ionized;
- for high temperatures ($10000^{o}K \leq T \leq 50000^{o}K$) in the case of a composition more metal-poor than the solar one Kurucz's models for $Z = Z_{\odot}$ can be used; Capuzzo-Dolcetta et al. (1983) in fact have shown by comparing model with $Z = Z_{\odot}$ and models with lower metal abundance in the temperature range $10000^{o}K$-$25000^{o}K$ that the differences between models with different metal content but same effective temperature, tend to decrease and become meaningless as temperature increases.

Kurucz's models of stellar atmospheres have been reckoned under the following assumptions:

1) local thermodynamic equilibrium (LTE),
2) parallel plane geometry,
3) hydrostatic equilibrium,
4) radiative or convective transfer of energy,

5) the molecular component is omitted in the equation of state.

6) microturbolence with ξ = 2 Km sec^{-1}.

7) the "blanketing" is taken into account.

The relaxation of these assumptions involves changes on the continuous flux:

a) Substitution of the LTE with non-LTE hypothesis produces an increase of the UV flux, a decrease of the infrared flux (IR), a larger Balmer jump (Fig. 3), and an increase of the amount of radiation subtracted by spectral lines (blocking) in the UV.

b) Introduction of a spherical geometry produces an increase of the IR flux and a decrease of the UV (the opposite effect of the non-LTE).

c) An increase of the microturbolence enhances the blocking effect.

The SEDs of Kurucz's models have been compared with observational data for the various type of stars, by several authors.

i) O - B stars: Remie and Lamers (1982) found that the effective temperatures and surfaces gravity derived from a given star by fitting different portions of the spectrum are often different, moreover the observed flux is higher for $\lambda \approx$ 2000-3600 A and lower for $\lambda \approx$ 1380-2000 A, and moreover the Balmer jump is smaller, these differences are the largest for I luminosity class stars. The discrepancies do not seem to be caused by the non inclusion of non-LTE and spherical geometry since their effects are balanced, very probably the line blocking is underestimated

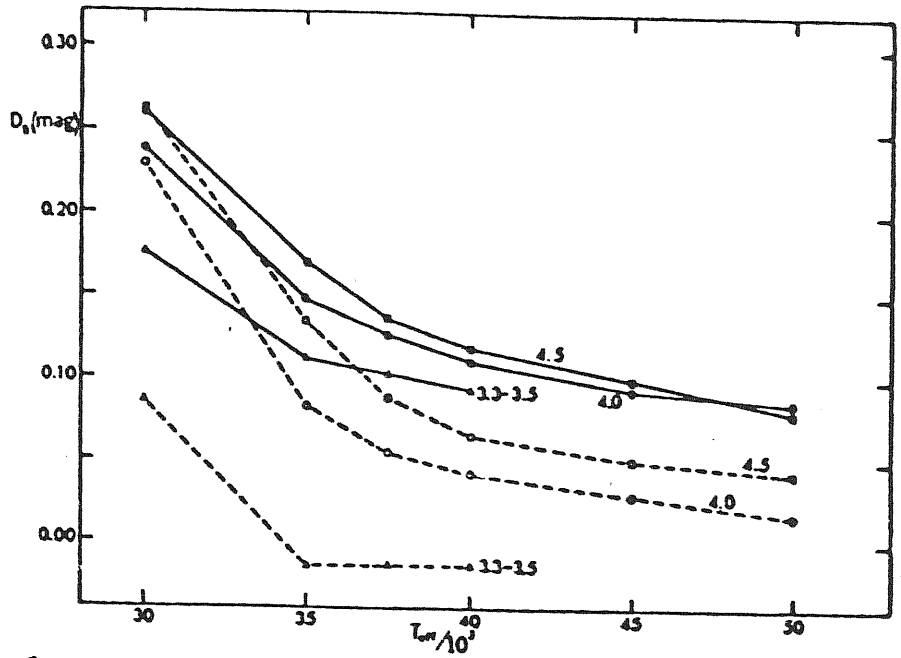

FIG. 3.—Balmer jump as a function of T_{eff}. The curves are labeled with the corresponding values of log g; solid curves with solid symbols denote non-LTE models, dashed curves with open symbols denote LTE models.

(Auer and Mihalas 1972)

in the models, and this can arise for two reasons: the microturbolence must be higher ($\xi \approx 10$-15 Km sec^{-1}) or some lines of double ionized metals have been neglected.

ii) B5 - A0 stars: Malagnini et al. (1983) found a good agreement between theoretical and observed SED in the optical region with $\Delta \log F_\lambda < 0.02$. There is instead some disagreement in the UV region between the model SED and those presented in the TD1 satellite altlas (Jamar et al. 1976, Macau-Hercot et al. 1978) (Fig. 4); it is not excluded however that TD1 data can be miscalibrated (Fig. 5) (Bohlin et al. 1980).

iii) A - F stars: Malagnini et al (1982) found that the models provide a realistic description of the observed spectra (Fig. 6); but the effective temperature derived from UV flux is smaller than that derived from optical flux. This fact can be due to an flux underestimation of the UV opacities.

iv) For cool stars the neglect of the molecular component in the equation of state raises some difficulties.

The most recent and refined evolutionary tracks for very massive stars imply effective temperatures as high as 150000^oK, although for a very small fraction of the total lifetime (10^5 yr.). For such models as far reproduction of the continuum is concerned one can use Kurucz's models when $T_{eff} \leqslant 50000^oK$. This approximation can be applied also to those models which, owing to the loss of a large amount of mass, have a surface composition deficient in H, as it turns out that atmospheric models of pure He, at high temperature, are not very different from the models with normal composition (Underhill 1980). For $T_{eff} > 50000^oK$ the

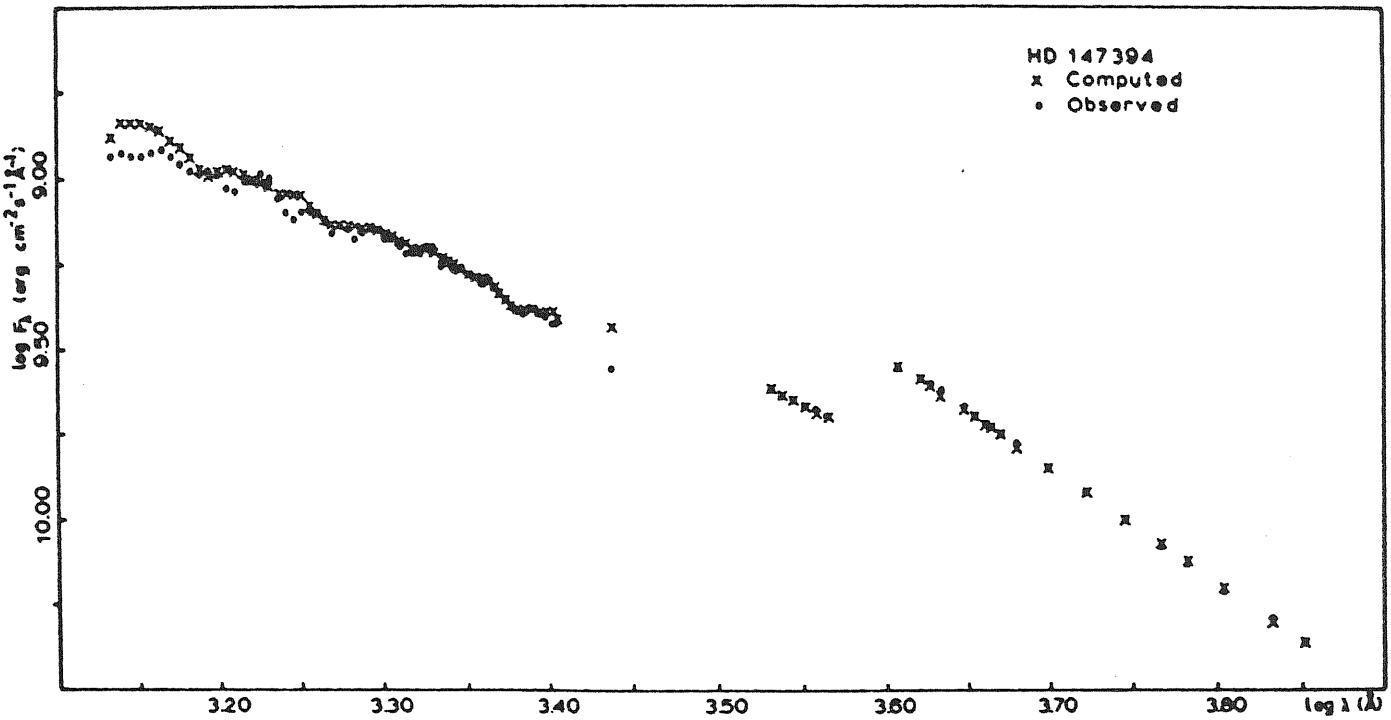

Fig. 4. The observed (●) and computed (×) $\log F_\lambda$ vs. $\log\lambda$ for HD 147394 (Malagnini et al. 1983)

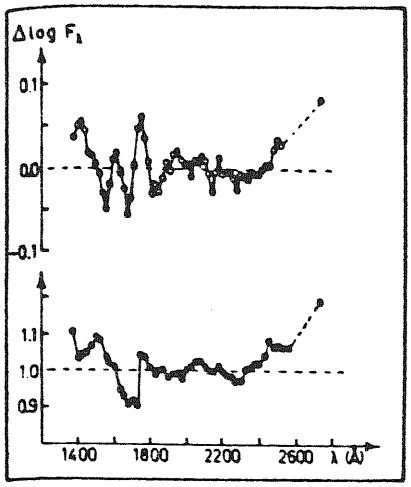

Fig. 5. The UV residuals (○) for HD 41692 are plotted, together with the correction factors (●) given by Bohlin et al. (1980) for S2/68 data of η UMa

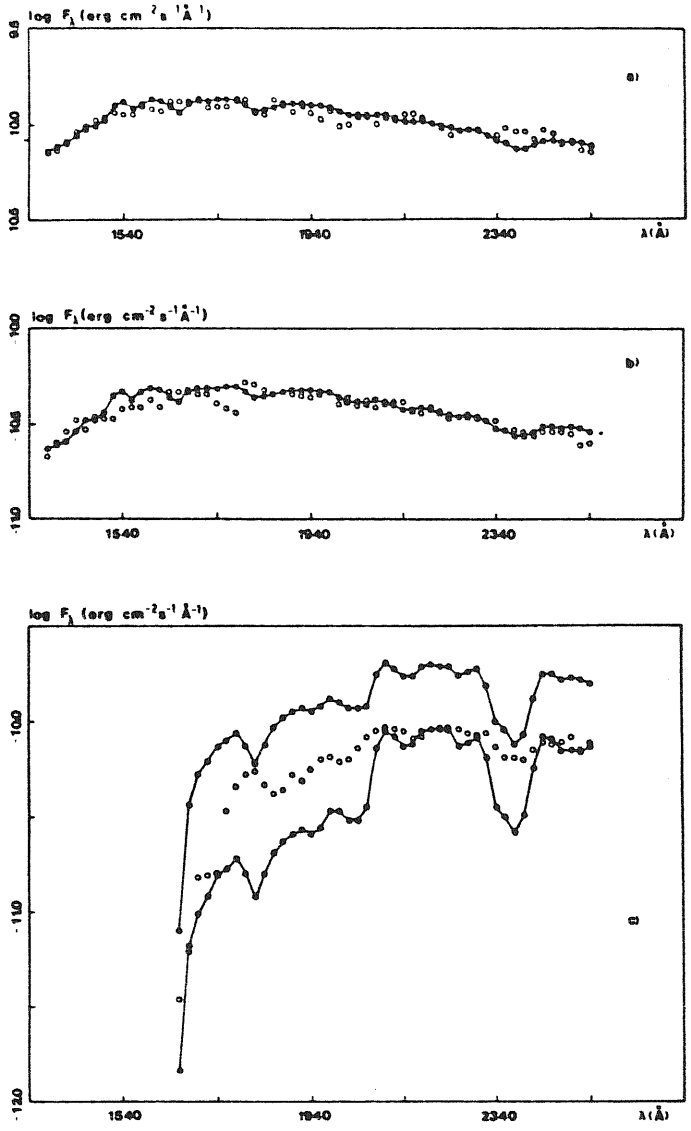

Fig. 6. Observed (circles) and computed (full line) spectra for: a) HD14055, example of good agreement; b) HD66664, example of intermediate agreement; c) HD432 for which no fits have been found (Malagnini et al. 1982).

black body emission curves can be a reasonable approximation since they fit very well both Kurucz's models for $T_{eff} \approx 50000^{o}K$ and the observed spectra of O type stars.

Alternatively to the models of stellar atmospheres one can use a library of observed stellar spectra which covers the required range of effective temperature, surface gravity and whose wavelength interval is sufficiently large. To build up a library of observed spectra the best material is offered by spectrophotometric observations which analyse the energy distribution in several points and within rather narrow bands so that the corresponding flux can be considered almost monochromatic. The observations most useful for an evolutionary synthesis are those at low dispersion, since the goal, at present, is to reproduce the behaviour of continuum without taking into account the detailed spectral features. Straizys and Sviderskiene (1972) have derived standard energy distribution in the optical region for several stars of different spectral types and luminosity classes by combining observations of several authors with atmospheric models. Spectrophotometric UV observations are presented by:

a) the Bright Stars Catalogue which gives monochromatic fluxes in 61 bands for 1971 stars observed by the TD1 satellite (Jamar et al. 1976, Macau-Hercot et al. 1978);

b) the UV Stellar Spectra Atlas of the OAO-2 satellite (Code and Meade 1979, Meade and Code 1980) with the fluxes of 330 bright stars corresponding to 120 bands in the wavelength range 1200 - 3580 A;

c) the IUE Stellar Spectral Atlas which covers the spectral region between 1150 - 3200 A.

The derivation of a stellar flux library from the collections of observations of different sources encounters several difficulties due to the uncertainty of the relations between the observed data and the theoretical quantities T_{eff} and g. The method generally adopted to compute these relations essentially consists in deriving from the atmosphere models some parameters and comparing them with the same observed quantities relative to several spectral and luminosity classes until the fit is obtained; in this way the required correspondence is obtained.

6. COSMOLOGICAL APPLICATIONS OF THE MODEL.

During their life the galaxies change continuously their stellar content. There are two basic mechanisms causing the stellar content of a galaxy to change, first stars continuously evolve and eventually die; second new stars appear in the galaxy. The evolution of stellar populations affects the integrated spectrophotometric properties; the change concern both the luminosity and the SED form.

When we observe distant objects we see their properties how they were at the moment in which the light rays started their path towards us. So when we want to test cosmological models and their parameters by means of observations of distant galaxies their evolution must be taken into account. Then the modelling of the spectral evolution of galaxies can be, in principle, a big

help in improving some knowledges of the universe.

The standard cosmological model depends on two parameters q_o and H_o whose determination is still largely uncertain. In general cosmological tests are not based on the observations of particular quantities, but rather rely on some correlations as: the Hubble's diagram, which links the apparent magnitude and the redshift; and the plot of the number of observed galaxies with a given apparent magnitude m against m itself.

In the following we will see how these relations are constructed and how galactic evolution enters in them.

6.1 The apparent magnitude redshift diagram (m - z).

For a given redshift (z) the cosmological model supplies:

a) The luminosity distance d_L, that is the distance estimated from the difference between apparent and absolute magnitudes. This relation cannot be derived in exact way but some approximation must be used

$$d_L = \frac{c}{H_o\, q_o^2} \{q_o z + (q_o - 1)[(1 + 2q_o z)^{1/2} - 1]\} \qquad \text{for } q_o \neq 0$$

$$d_L = \frac{c}{H_o}\, z\,(1 + z/2) \qquad \text{for } q_o = 0.$$

b) The look back time τ.

$$\tau = t_o - t_z$$

and

$$H_o t_z = \frac{(1 + 2q_o z)^{1/2}}{(1 - 2q_o)(1 + z)} + q_o\,(2q_o - 1)^{-3/2}\; \Lambda\left(\frac{1 - q_o(1 - z)}{q_o(1 + z)}\right)$$

$$\Lambda(x) = \begin{cases} \arccos(x) & \text{for } q_o > 0.5 \\ (-1)^{1/2} \operatorname{arccosh}(x) & \text{for } q_o < 0.5 \end{cases}$$

$$H_o t_z = 2/3\ (1 + z)^{-3/2} \qquad \text{for } q_o = 0.5.$$

c) The models of galactic spectral evolution supply the SED as a function of the age and the morphological type of galaxies

$$F_{\lambda_1}\, d\lambda_1 = F_{\lambda_1}(\tau,\ \text{galaxy-type})$$

it is then possible to derive:

i) the apparent flux

$$\log f_{\lambda_1} = \log F_{\lambda_1} - 2 \log d_L + C$$

where C is constant;

ii) the flux into a photometric band

$$f_B = \int_{-\infty}^{+\infty} S_B(\lambda)\ f\left(\frac{\lambda}{1+z}\right)\ \frac{d\lambda}{1+z}$$

where $S_B(\lambda)$ is the response function of the photometric system;

iii) and the apparent magnitude

$$m_B = -2.5 \log f_B + C_B.$$

Fig. 7 shows the dependence of the (m - z) relation from q_o, and Fig. 8 shows (m - z) relation including spectral evolution (Bruzual 1981). Since according to the models the luminosity of galaxies decreases with the age to account of evolutionary effects decreases the estimated value of q_o.

The method of deriving the model parameters based on the Hubble relation do not yield reliable estimates of q_o, in fact it is affected by the following uncertainties:

1) The Scott effect (Sandage 1961): if the galaxies used are the brightest galaxies of the clusters, at high z the richest clusters whose brightest galaxies are most luminous are most

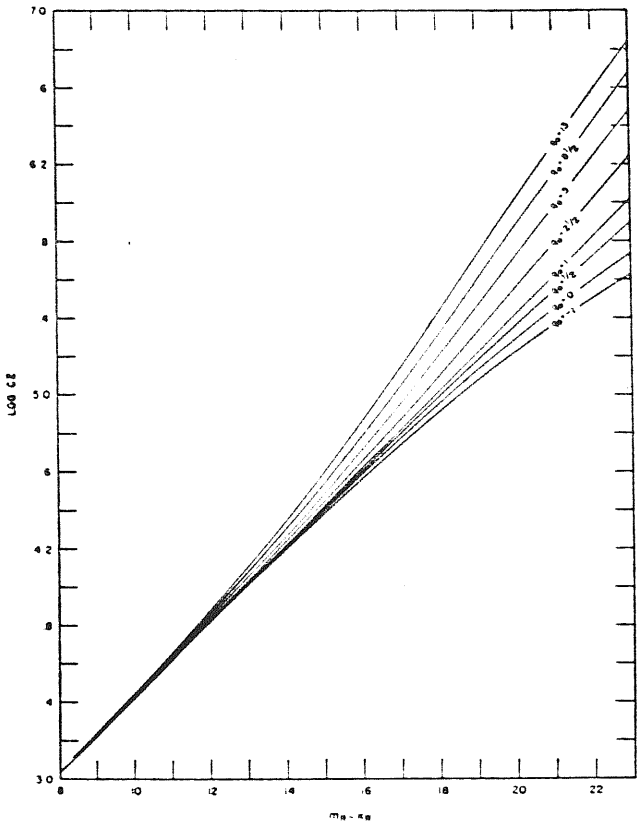

Fig. 7. The redshift-magnitude relation for various values of the deceleration parameter. The curves have been normalized to agree with the observations at bright magnitudes (Sandage 1961).

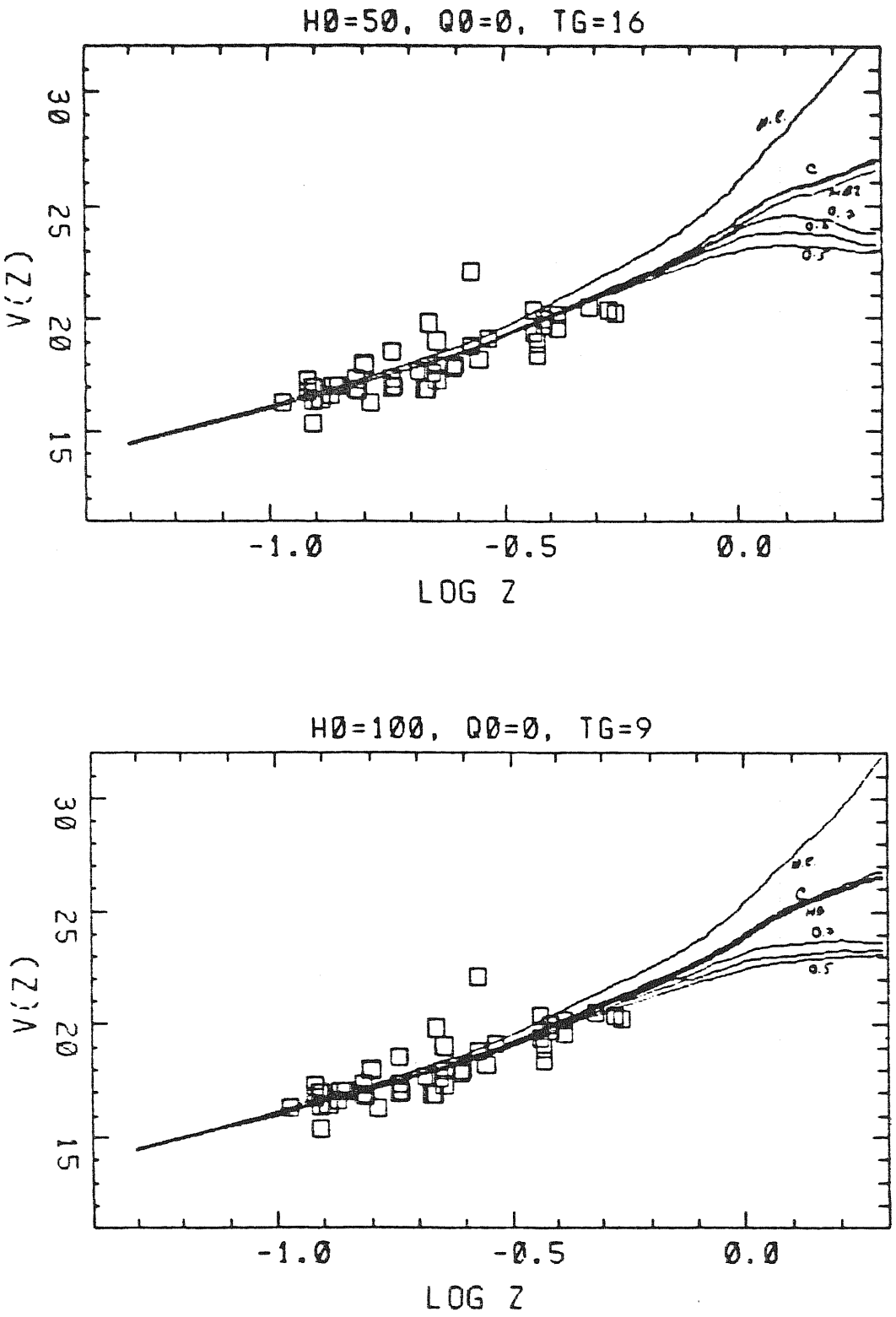

Fig. 8. The redshift-magnitude relation including evolution (Bruzual 1981). The data points are from (Kristian et al. 1978).

easily selected.

2) The definition of the magnitude is affected by the aperture of the instrument used: at different distances the aperture includes different portions of the galaxies thus affecting the evaluation of their total luminosity.

3) The cannibalism effect: collisions between galaxies are a very frequent phenomenon, so the brightest members of a cluster can be the result of iterated actions of cannibalism and can have an evolution completely different than that caused only by the evolution of the stellar content; this anomalous evolution could increase the luminosity, contrary to what normally happens. The effect of the cannibalism partly can balance the effect of the luminosity evolution making the Hubble relation almost insensitive to the luminosity changes; this fact however it not an advantage since Tinsley (1981) has shown that the m - z relation could become almost independent of q_0.

4) Difficulties in the z determination.

6.2 The count-apparent magnitude diagram (N_m - m).

A more reliable method for the determination of the parameter q_0 is based on the N_m - m relation, which is not affected by the problems concerning the brightest members of the clusters. This method needs however a more complex procedure for the evaluation of the theoretical relation.

From the cosmological model we can derive:

a) The luminosity distance (d_L).

b) The look back time (τ).

c) The volume element (dV).

$$dV = \frac{4\pi c^3}{H_0^3 (1+z)^6} \begin{cases} \dfrac{\{q_0 z + (q_0 - 1)\,[(1 - 2q_0 z)^{1/2} - 1]\}^2 \; dz}{q_0^4\,(1 + 2q_0 z)^{1/2}} & \text{for } q_0 \neq 0 \\ z^2\,(1 + z/2)^2\, dz & \text{for } q_0 = 0 \end{cases}$$

From the spectrophotometric evolution we can obtain:

d) the relation between the absolute magnitude M_i of a galaxy at a given redshift z and the absolute magnitude M_0 that the same galaxy would have in the our neighbourhoods, that is at zero red shift.

The observations provide:

e) The luminosity function of the galaxies in our neighbourhood

$$\Phi(M_0) \qquad \text{or} \qquad \Phi(L_0)$$

Schechter (1976) finds the following form:

$$\Phi(L)\, dL = \Phi^*\, (L/L^*)^{\alpha}\, e^{-L/L^*}\, d(L/L^*)$$

with Φ^* parameters. An equivalent form is

$$\Phi(M)\, dM = 0.92\, \Phi^*\, X^{1+\alpha}\, e^{-X}\, dM \quad \text{with} \quad X = 10^{0.4(M-M^*)}$$

the parameters Φ^* M^* and α have been determined by several authors and their values are shown in the following table IV.

Table IV.

α	M^*_j	$\Phi^*(Mpc^{-3})$	Source
-1.25	-21.1	5.0E-3	Schechter 1976
-1.0	-21.1	1.4E-3	Turner and Gott 1976
-1.24	-21.28	2.2E-3	Felten 1977
-1.24	-21.17	2.9E-3	Huchra 1978
-1.0	-21.0	1.8E-3	Davis et al. 1979
-1.10	-21.1	2.3E-3	Kirschner et al. 1979
-1.03	-20.9	-	Tamman et al. 1980
-1.0	-20.9	1.4E-3	Durham survey

the mean values are $\alpha = -1.11 \pm 0.12$ and $M^*_j = -21.1 \pm 0.14$ (Ellis 1982). The luminosity function derived by these values is

shown in Fig. 9 together with some observational points. The luminosity function is however affected by some uncertainties. First, the number of luminous galaxy in our neighbourhood is small and consequently our sample can be affected by fluctuations; second, the clusters data can be contaminated by the background. However some authors have found (Bruzual and Kron 1980, Tinsley 1980) that the correct form of $\Phi(L)$ is not important for the present purpose, what is needed is the quantity:

$$M\dagger_m = \frac{\int M\, P(m|M)\, dM}{\int P(m|M)\, dM} \qquad \text{with } P(m|M) = \int \Phi(M)\, dV(z,q_o)$$

$M\dagger$ is nearly independent of m, then $M\dagger_m = M\dagger$ = constant.

f) The local density of galaxies (N_o). This quantities is required for the normalization of $\Phi(M)$. Also N_o is uncertain: overestimation can arise from the presence of nearby clusters; N_o is preferably estimated from objects at a suitable distance rather than in our neighbourhood in order to avoid the inclusion in the sample of clusters which can bias the results. However the exact value of N_o is not required since the quantities N_m/N_o can be used (Tinsley 1980, 1981).

g) the mix of galaxies of various type: estimates for the relative frequencies are discordant (see table V)

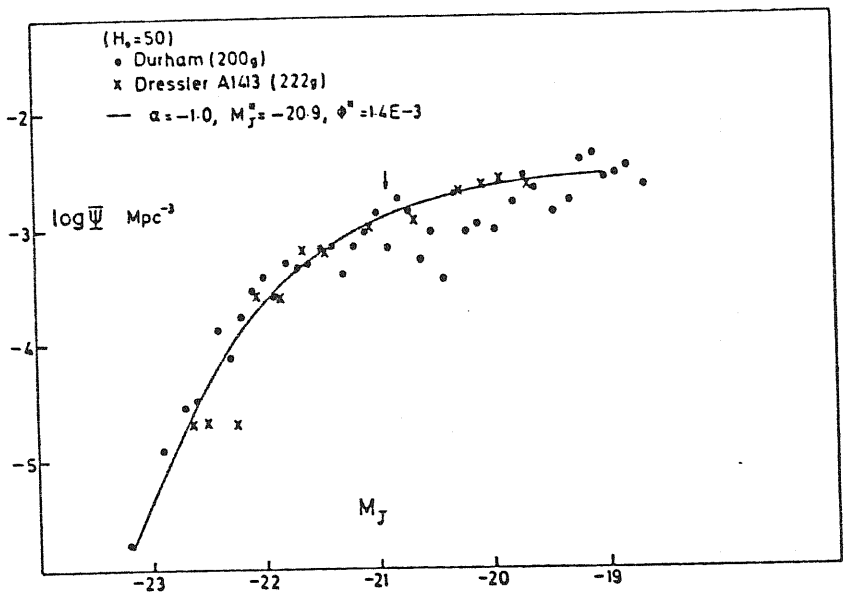

Fig. 9. Differential galaxy luminosity function in J passband (Ellis 1982).

Table V.

E/SO	Sabc	Scdm	Source
28	46	26	Durham J<16.5
23	39	38	Hubble 1926
23	34	43	van den Bergh 1960
28	32	40	Sandage 1961
24	52	24	Dostal 1979
45	27	28	Kirschner et al. 1979

Some authors derive the mix by imposing that the observed colour distributions must be reproduced (Kron and Bruzual 1980).

The N_m - m relation can be obtained from all the previous elements. For a fixed value of m and for any z we have:

$$\tau = \tau(z|q_o,H_o)$$

$$d_L = d_L(z|q_o,H_o)$$

$$M_1 = M_1(m,z|q_o,H_o)$$

from the spectral evolution

$$M_o = M_o(M_1,\tau)$$

from which we get

$$M_o = M_o(m,z|q_o,H_o)$$

The luminosity function can be expressed in terms of z

$$\Phi(m,z|q_o,H_o)(dM_o/dz)\,dz$$

and so

$$N_m\ \Delta m = \int_0^\infty N_o/4\pi\ dV/dz\ \Phi(m,z|q_o,H_o)\ (dM_o/dz)\,dz\ \Delta m.$$

The N_m - m diagram derived by Ellis 1982 is presented in Fig. 10.

There is uncertainties again due to contamination by stars and to the definition of the magnitude; in fact the fraction of light within a given isophote decreases as z increases.

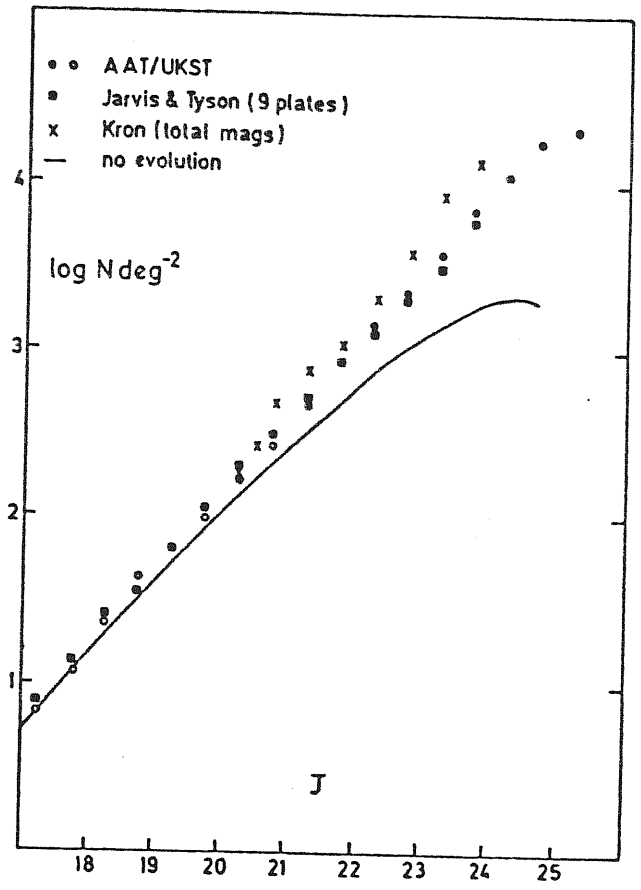

Fig. 10. Differential J number magnitude counts in 0.5 mag bins. (Ellis 1982)

7. THE SPECTRA OF STELLAR GENERATIONS.

Relation (1) can be written in the following form:

$$F_\lambda(T) = \int_0^T B(t)\, f_\lambda^*(\tau)\, dt$$

where

$$f_\lambda^*(\tau) = \int_{m_L}^{m_U} \phi(m)\, f_\lambda(m,\tau,Z(t))\, dm$$

is the integrated monochromatic flux of a stellar generation of age τ and metal abundance Z(t). Therefore the computation of a galaxy model can be performed in two steps: a) calibration of the integrated SED of the stellar generations of different age; b) computation of the galaxy integrated spectrum as superposition of the contributions of all the generations, each of them weighted by the function B(t). This fact suggests that the first test to verify the agreement of the models with the observations should be the comparison of the integrated spectra of single generations with the observed spectra of star clusters. This two-step procedure is not essential, still the spectra of the single generations can be derived by choosing a birth rate defined by an impulsive function.

7.1 Young stellar generations.

In the following a series of population I models with $t<10^9$ yr will be described. They have been derived under the following assumptions:

d) the metal abundance is Z=0.02;

e) the initial mass function is the Salpeter function with α=2.35.

The models have been grouped in order of increasing age.

1) $1x10^6 < t < 3x10^6$. All the stars are supposed to belong to the Main Sequence: this is true for the more massive ones since their MS lifetime is larger than $3x10^6$ yr. Stars of low mass which are still in the contraction phase prior to the H ignition, have been treated as ZAMS stars; their contribution is not relevant to the total light in any wavelength region considered. The integrated spectrum is very similar to the spectrum of a hot star: the monochromatic flux f_λ^* is a monotonically decreasing function of λ.

2) $3x10^6 < t < 8x10^6$ (the evolved stars have masses in the range $29 < m < 100\ M_\odot$). f_λ^* is still monotonic; its slope however is smaller both owing to the disappearance of the most massive stars from the Main Sequence and because there is now a number of evolved stars in the region of low and intermediate temperatures.

3) $8x10^6 < t < 7x10^7$ (mass of evolved stars: $5.6 < m < 29\ M_\odot$). The Balmer discontinuity and some H lines appear on the spectrum and gradually become more marked. f_λ^* shows a maximum in the UV region which moves at high wavelengths (still remaining in the far UV), a minimum below the Balmer discontinuity at λ=3650 A and moreover a further relative maximum at λ=3850 A.

4) $7x10^7 < t < 3x10^8$ (mass of evolved stars: $3.1 < m < 5.6\ M_\odot$). In the spectrum the Balmer discontinuity and the lines are clearly evident. The two maxima at first tend to be level and then the maximum in the optical region at λ=3850 A becomes prominent. The UV flux progressively decreases, as the hottest

stars gradually evolve from the Main Sequence becoming colder.

5) $3x10^8 < t < 8x10^8$ (mass of evolved stars: $2.2 < m < 3.1\ M_\odot$). The Balmer lines the discontinuity still appear, other features however are present: the lines of the ionized metals FeII, SiII etc. The maximum in the optical region becomes more prominent and moves at higher wavelengths; the other maximum in the UV region becomes fainter.

In Fig. 11 some spectra are presented with the purpose of showing how they evolve when the generation ages. In a more synthetic way two fundamental types of spectra can be distinguished: a) spectra of very young generation with a monotonically decreasing monochromatic flux, these spectra are very much like the spectra of an O star and clearly the integrated light is dominated by such stars; b) spectra of intermediate generation in which the SED exibits two maxima and the Balmer discontinuity is always present; the spectra of this generation is dominated by A and F stars, whose spectra also show these features.

Models have been computed also by changing the exponent of the initial mass function. Adopting α=3 the new models, in respect to the previous set, exhibit the following behaviour:

a) the difference between two models with different α and the same age is more marked when $t < 10^7$ yr. due the different relative number of massive stars; this difference tends to disappear as the generation grows older;

b) owing to the lower relative number of massive stars in the case α=3 which allows the emergence of the contributions of less

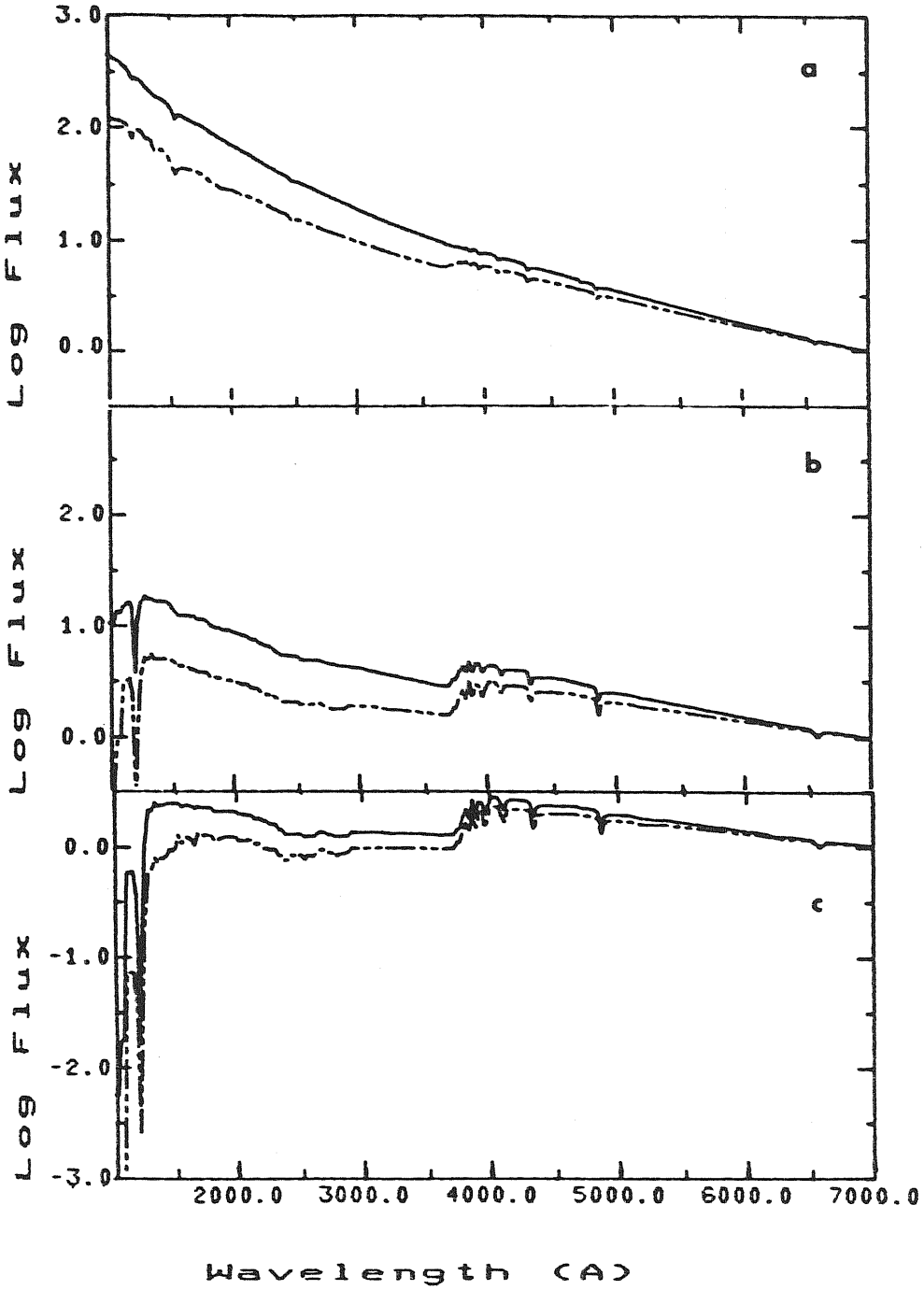

Fig. 11. Generation models for several ages (million years): a) t=1 and 8, b) t=40 and 150, c) t=300 and 500.

massive stars, the Balmer discontinuity appears in the integrated spectrum earlier than in the other case.

The best candidates for a test of these models are the globular-like clusters of the Magellanic Clouds. The HR diagram for many of these clusters is available, in this way we can derive independent estimates of the age; moreover several determinations of their chemical composition are also published. Searle et al. (1973, SWB) have developed a classification of the clusters of the LMC based on two reddening-free parameters derived from Gunn's photometric system (Thuan and Gunn, 1976); according to this classification the clusters are arranged in a sequence along which both age and metal content are changing. The correlation between the types defined by SWB and the age is still uncertain and different age intervals are defined for the classes from different authors (e.g. Cohen 1982, Hodge 1983).

Cohen et al. (1984) have derived UV spectroscopic observations with the IUE for 17 globular clusters of the LMC which cover the whole range of the SWB classes. From this sample we have excluded those clusters which do not belong to the age range here considered, for the remaining 14 the colour C1=(1345-3150) and C2=(1750-2670) have been derived from their Table I and have been corrected for reddening in the same way as described by the authors, namely by separating the absorption due to our Galaxy from that correspondent to the LMC.

Fig. 12 shows the two colour diagram of the clusters; the theoretical calibration line, which has been derived from the synthetic spectra previously analysed, is also plotted (full

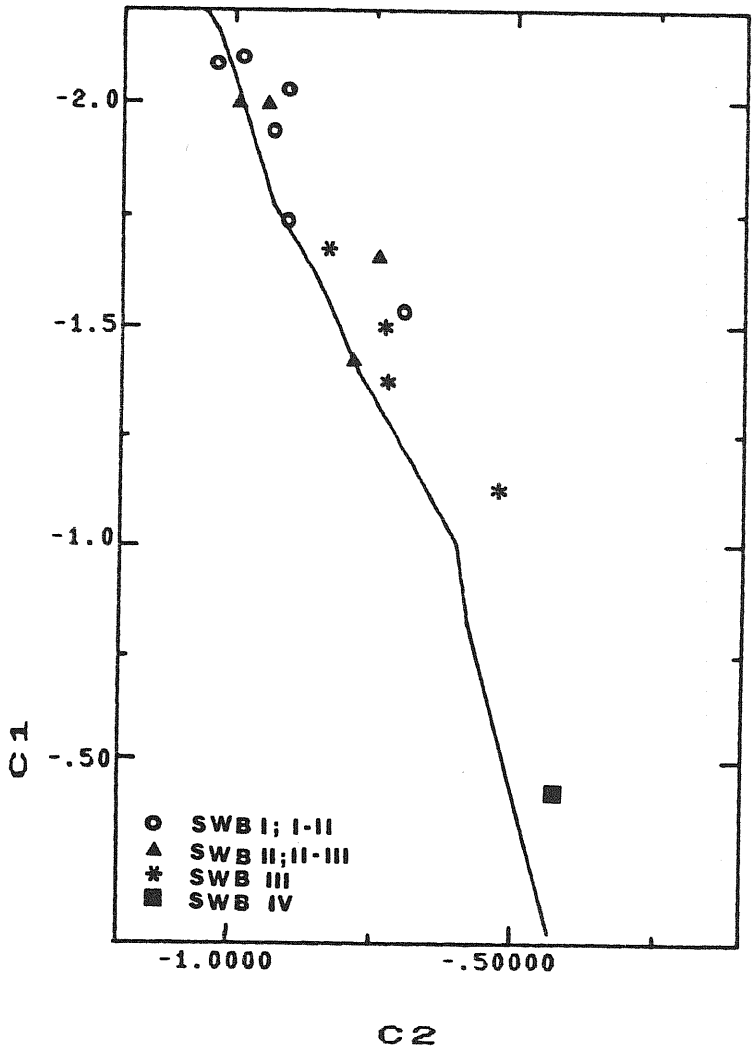

Fig. 12. UV two-colour diagram for LMC clusters.

line). From the figure it results that, neglecting the subdivision in SWB classes, the observed colours, after correction for reddening, are in reasonable agreement with the theoretical predictions and the dispersion is small. However taking into account the SWB types, we note that there is a non negligible mixing of objects of different types. This fact may have several causes: a) the evaluation of the reddening is not correct, a better estimate of this correction could move the objects in the right position since the reddening line is almost parallel to the theoretical locus; b) there are errors in the observations; c) the criteria according to which clusters are put into classes are such that only to a first approximation do the SWB types correlate with age. In particular the cluster NGC2100 [C1=-1.55, C2=-0.71] deviates significantly from the average positions of the sample clusters belonging to the same type. By making use of the theoretical colour-age relations average values of the age have been derived for the first four SWB classes.

TABLE VI.

SWB	C1	C2	$t(10^7 yr)$	$t(10^7 yr)$
I	-2.11	-1.00	3.5	1.4
II	-1.54	-0.79	10.4	5.0
III	-1.52	-0.75	10.6	7.5
IV	-0.94	-0.65	19.2	---

The dispersion in age, shown in column 5, is computed from the dispersion of the observed colours and does not take into account the possible uncertainties connected with the theoretical calibrations; moreover, due to the small number of clusters considered, it is only indicative. The whole sample has been compared by Cohen et al (1984) with theoretical models but, since

their models have ages ranging from $2x10^8$ to $1.2x10^{10}$, their analysis mainly refers to the last SWB types and there is only a small overlap with the models here considered.

Cohen et al (1984) have also shown the UV spectra of four clusters. These spectra are presented in Fig. 13 with model spectra chosen in order to give the best fit with the observed spectra. Although no attempt has been made to correct the cluster spectra for reddening, the agreement is rather good and the continuum is very well reproduced with the exception of the very far UV (λ < 1200 A).

The spectrum of the cluster NGC2004 is fitted by a synthetic spectrum with age intermediate between $4x10^7$ and $7x10^7$ yr (from the UV colours we derived $t=3x10^7$ yr). Hodge (1983) derives from the HR diagram an age of $8x10^6$ yr and Cohen (1982) estimates an average age of 10^7 yr for SWB type I clusters. The cluster NGC1711, according to the fitting with the present models is $7x10^7$ years old (and from UV colours is $1.4x10^7$ years old). According to Hodge (1983) SWB II clusters have $1.3x10^7<t<4x10^7$ while according to Cohen (1982) $t=5x10^7$ yr.

For the cluster NGC1866 we derive from the fitting of the spectrum an age intermediate between $1.5x10^8$ and $3x10^8$yr, from the UV colours $2x10^8$ yr; the age, estimated from the HR diagram (Hodge 1983) is $8x10^7$ and Cohen for SWB III clusters gives $t=5x10^8$ yr. The cluster NGC1856 is fitted by a synthetic spectrum of a generation $5x10^8$ years old; from the HR diagram an age is derived of $1.2x10^8$ yr, while Cohen (1982) derives for SWB IV clusters an age of 10^9 yr.

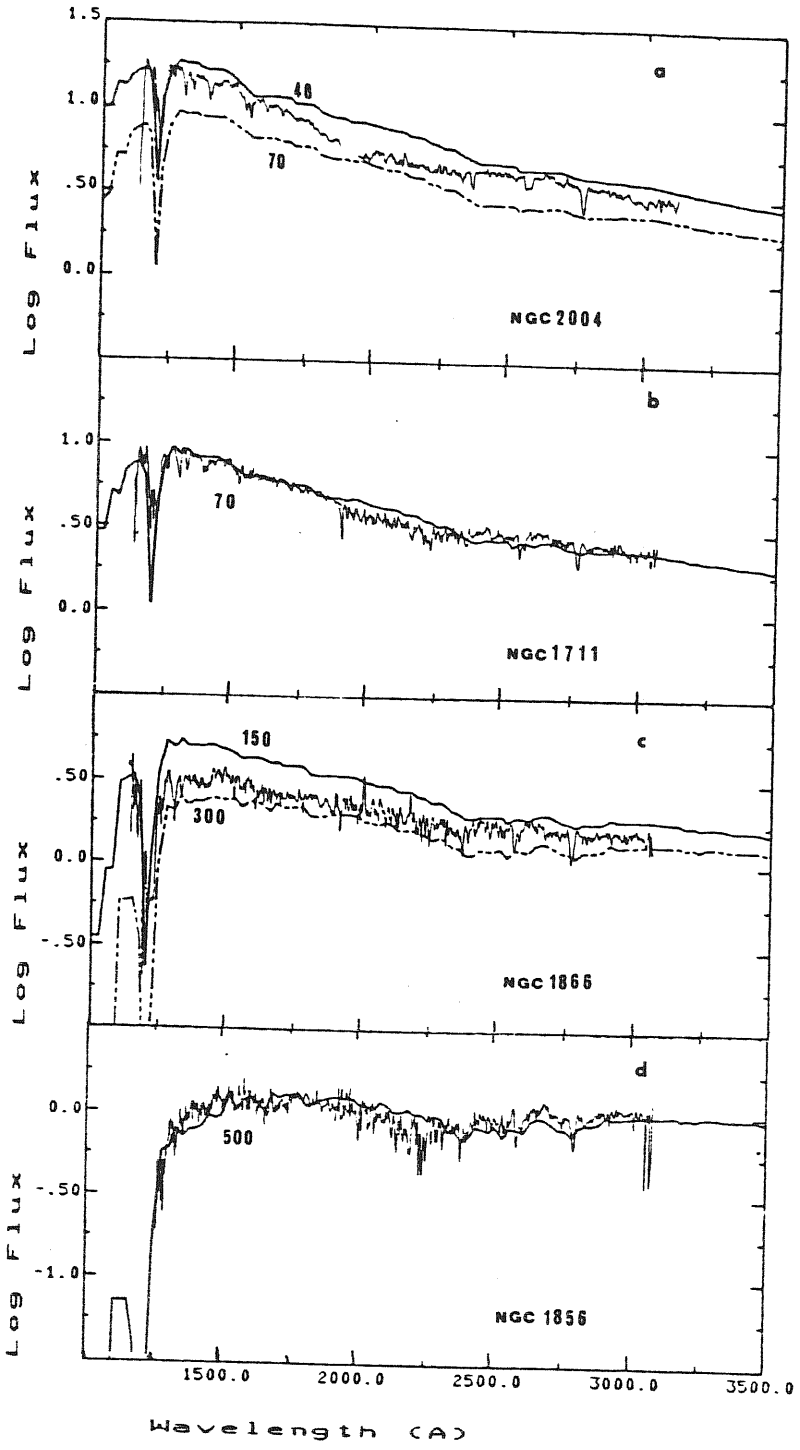

Fig. 13. Spectra of some young clusters (from Cohen et al. 1984) compared with models. Figures give the model age in 10^6 yr.

7.2 The spectra of old stellar generations.

Preliminary models of old stellar generations ($t > 10^9$ yr) have been computed for two chemical compositions: a) Y=0.30 $Z=10^{-2}$, b) Y=0.30 $Z=10^{-4}$.

7.2.1 Integrated spectra with $Z=10^{-2}$.

These have been collected in three groups according to their age: 1) $1x10^9 < t < 4x10^9$. The monochromatic flux in the UV region gradually decreases. The maximum in this region moves beyond the discontinuity at λ=2800 A due to MgII; moreover there are present the absorption features of FeII, SiII, etc. In the optical region the Balmer lines are weaker and weaker and tend to disappear.

Fig. 14a shows the spectrum of the generation $2.x10^9$ years old as representative of the group. The same figure also presents the spectrum from which the contribution of the He burning stars has been subtracted. As is well known, in the case of Pop. I, these stars occupy in the HR diagram the "clump" (Cannon 1970). The two spectra are not very different, however the clump stars increase the whole flux and reduce the slope of the spectrum in the red region.

2) $4x10^9 < t < 1.2x10^{10}$. The UV flux still decreases, being produced by the emission of the hottest main sequence stars. The absorption lines of FeII and SiII are still evident; in the optical region the flux has a maximum which, as the age

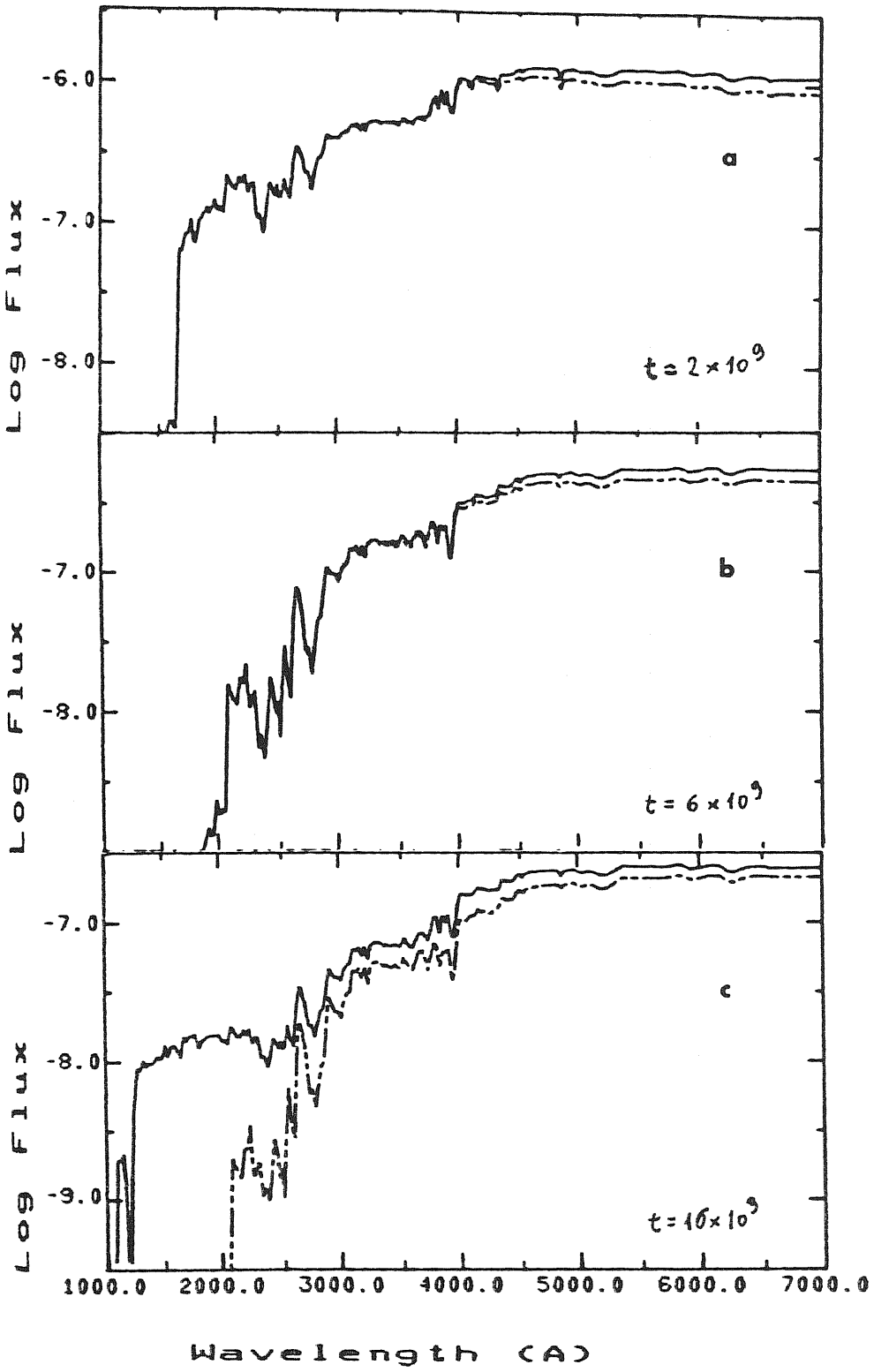

Fig. 14. Spectra of old generations with $Z=10^{-2}$. The lower curve of each panel gives the SED computed without clump stars.

increases, moves towards the red region.

Fig. 14b shows the spectrum of the generation with $t=6x10^9$ yr with and without the contribution of clump stars. In this case also the inclusion of clump stars tends to flatten the monochromatic flux in the red region. The difference between the two spectra is small compared with the previous case: this derives from the reduced ratio of clump stars to the total number of red stars (stars in phase of shell H burning and core He burning) (Barbaro and Pigatto 1984).

3) $1.2x10^{10} < t < 1.6x10^{10}$. In the far UV region the monochromatic flux reverses the trend till now observed and begins to increase with age. The reason for this behaviour is that the clump now changes into a proper HB, gradually populated by hot stars. The flux from these stars opposes the gradual decrease of the UV flux from the stars of the MS turnoff point as the generation grows older. The temperature of the stars during the core He burning, for the two considered compositions, are shown as function of the age in Fig. 15. The extension of the HB is defined in such a way as to include 90% of the stars, leaving outside 5% from both sides.

In the optical region the H and K lines of CaII are present. In Fig. 14c the spectrum of the generation $1.6x10^{10}$ years old is shown; the lower curve is the spectrum when He burning stars are included: the difference between the two curves clearly indicates that HB stars are responsible for the flux in the region $1000 < \lambda < 2500$A.

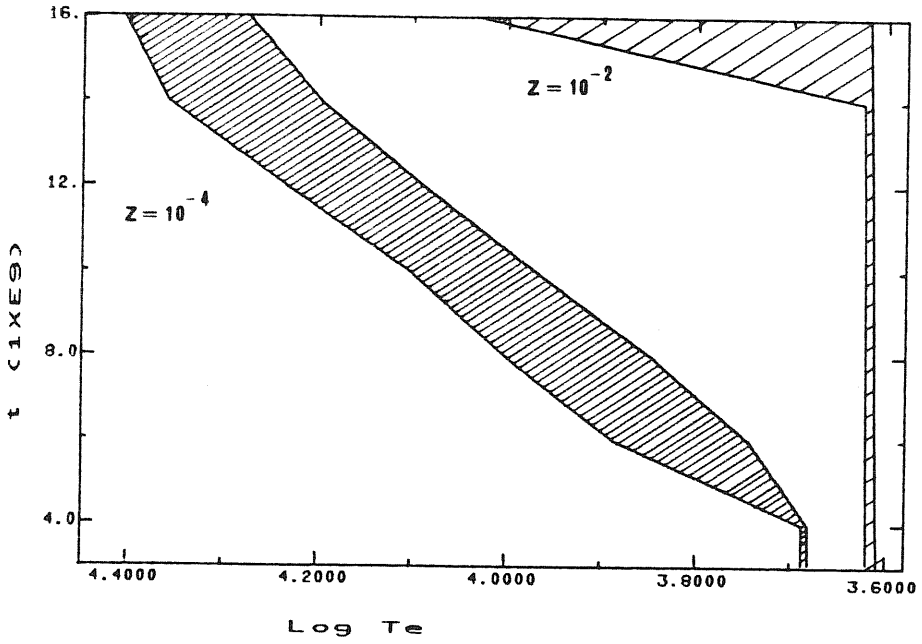

Fig. 15. Extension of the HB as function of age.

7.2.2 Integrated spectra with $Z=10^{-4}$.

1) $1x10^9 < t < 5x10^9$. In the far UV the monochromatic flux quickly increases with λ , beyond the Ly_α the continuum flattens. The Balmer discontinuity and some lines of the same series are present.

In Fig. 16a the spectra of the generation with $t=2x10^9$ and $t=4x10^9$ are shown; from the comparison of the two curves it turns out that the UV flux decreases as the age increases: this flux is produced by the stars of the MS turnoff point while the HB stars, having low effective temperatures, do not emit appreciably in the UV (cf. Fig.15).

2) $5x10^9 < t < 9x10^9$. At first the decrease of the UV flux continues but at $t=8x10^9$ the HB begins to extend towards high temperatures and its stars radiate significantly in the UV, thus increasing the flux.

Fig. 16b presents the spectral distribution for the generation $t=8x10^9$ yr.

3) $9X10^9 < t < 1.2x10^{10}$. Compared to the optical the UV flux increases and a maximum appears at λ=1250 A; just to the right of this maximum there is a large plateau extending up to 3500 A. There is also a second maximum at about 4000 A. The flux increases as the age increases.

4) $1.2x10^{10} < t < 1.6x10^{10}$. Qualitatively these spectra are similar to those of the previous group; however the intensity of the Balmer lines and the discontinuity decreases, while the maximum in the UV grows larger and moves at the left of the

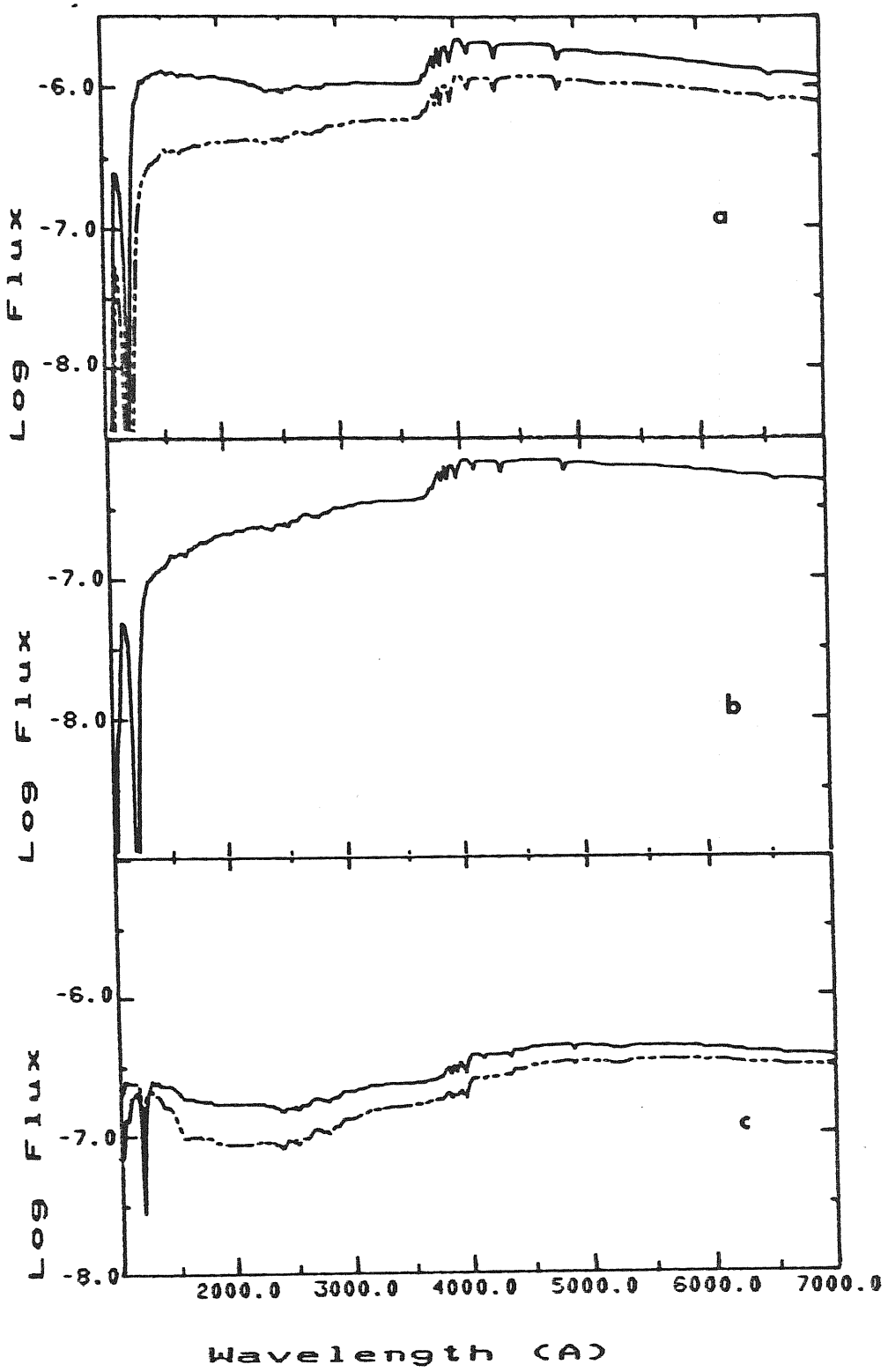

Fig. 16. Spectra of old generations with $Z=10^{-4}$: a) t=2 and 4; b) t=8; c) t=12 and 16 (ages are in 10^6 yr).

Ly_α line. Fig. 16c shows the spectra with $t=1.2x10^{10}$ and $t=1.6x10^{10}$ yr.

In Fig. 17 the spectrum with $1.6x10^{10}$ yr (upper curve) is compared with the spectrum obtained when HB stars are omitted. The HB, in this case, is populated by hot stars with a strong emission in the UV. For λ>3000 A the two spectra are similar, this showing that HB stars are too hot to emit significantly in this region.

It may be of interest to compare the spectra of two generations of the same age but different metal content. In the case of $t=2x10^9$ yr (Fig. 18a) the monochromatic flux in the far UV (λ < 1500 A) is much larger in the metal-poor spectrum and the difference decreases as λ increases and vanishes for $\lambda \simeq$ 5000 A. The different behaviour in the UV region is not ascribable to the HB which is red in both cases (cf. Fig. 15) but to the different temperature of the brightest MS stars. Fig. 18b shows the spectra with $t=8x10^9$ the relative behaviour is qualitatively similar to that of the previous case: the monochromatic flux of the model with $Z=10^{-2}$ begins to decrease, as the wavelength decreases, earlier than in the model with $t=2x10^9$ yr and this depends on the different temperature of MS turnoff stars in the two cases. Moreover in the UV the difference between the two spectra is still larger than in the previous case since now the UV flux is contributed also by the HBs, which have different extensions: HB stars of the model with $Z=10^{-2}$ being red while those of the model with $Z=10^{-4}$ are blue. The Fig. 18c refers to the generations with $t=1.6x10^{10}$ yr. There is still a difference in

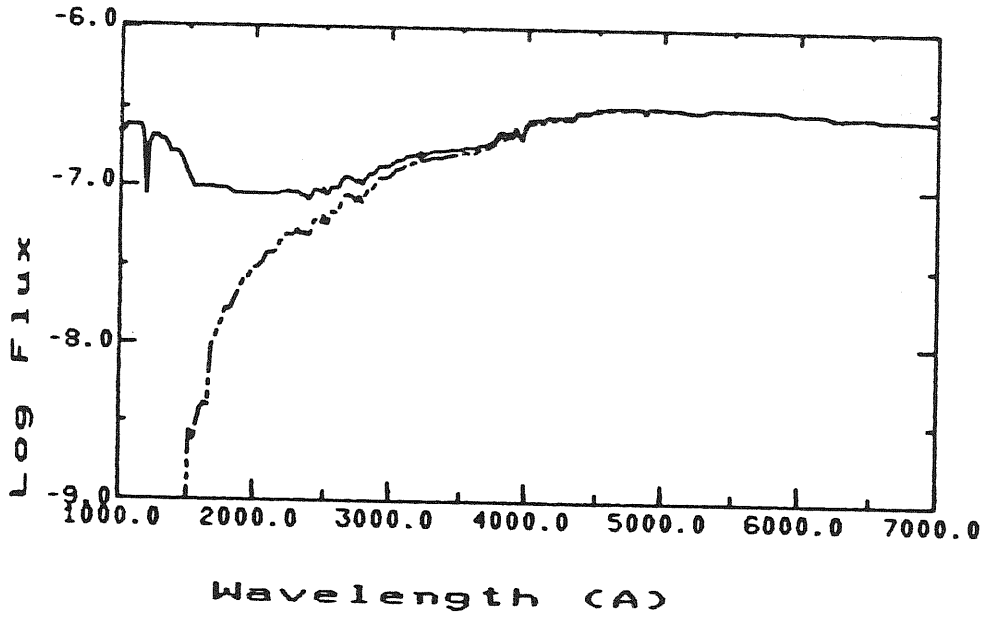

Fig. 17. SED of the generation $Z=10^{-4}$ and $t=1.6\times10^{10}$ yr (upper curve). Lower curve gives SED when HB stars are neglected.

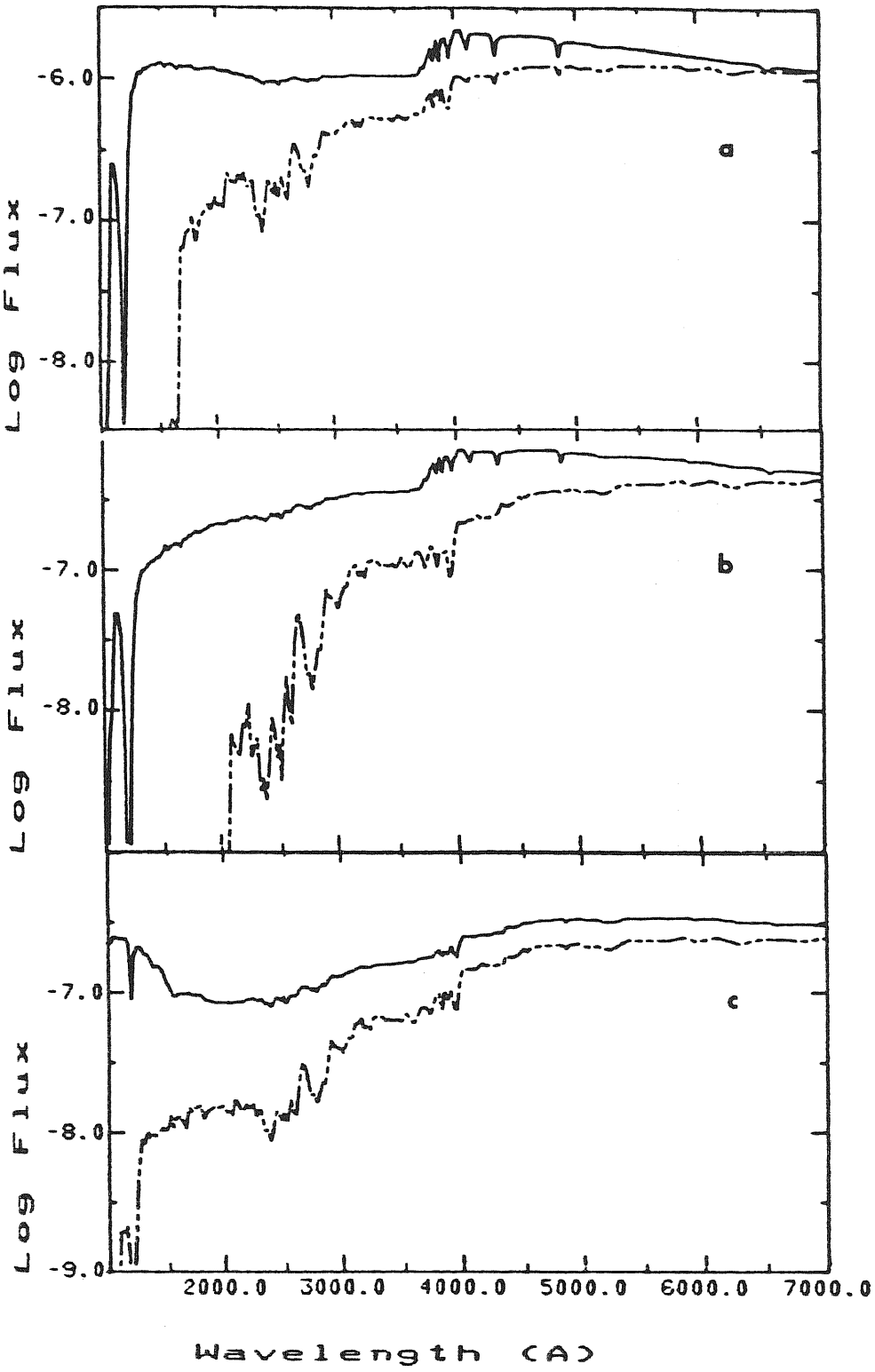

Fig. 18. Comparison of generations with same age and different Z: a) $t=2x10^9$; b) $t=8x10^9$; c) $t=1.6x10^{10}$.

the UV portion of the spectrum:this is partly due to the MS stars and partly to the HB which extends, although to a different extent, up to the blue. While the monochromatic flux of the case $Z=10^{-4}$ has a minimum for λ = 2000 A and then increases as λ decreases, the spectrum with $Z=10^{-2}$ continuously decreases as λ decreases: this difference in the far UV spectrum arises from the behaviour of the bluest HB stars.

The energy distributions of old generations have been tested by comparing them with the spectral distribution of globular clusters. These have been obtained from the ANS observations of de Boer (1985) who gives the average fluxes corresponding to 13 wavelengths (in several cases this number is smaller) covering a wavelength interval from 1550 A to 5500 A for many globular clusters. For some of them de Boer's data have been supplemented with Faber's data (1973): in this case the energy distribution extends up to 7400 A. Moreover for several of the considered clusters Nesci (1981 and private communication) has derived IUE ultraviolet spectra.

Table VII gives for each of the analysed clusters the metal abundance taken from Harris and Racine (1979) and HB types from Dickens (1972). In Fig. 19 the SEDs derived from the de Boer's observations, corrected from reddening according to Seaton (1979), and the theoretical curves which give for each case the best fit are shown.

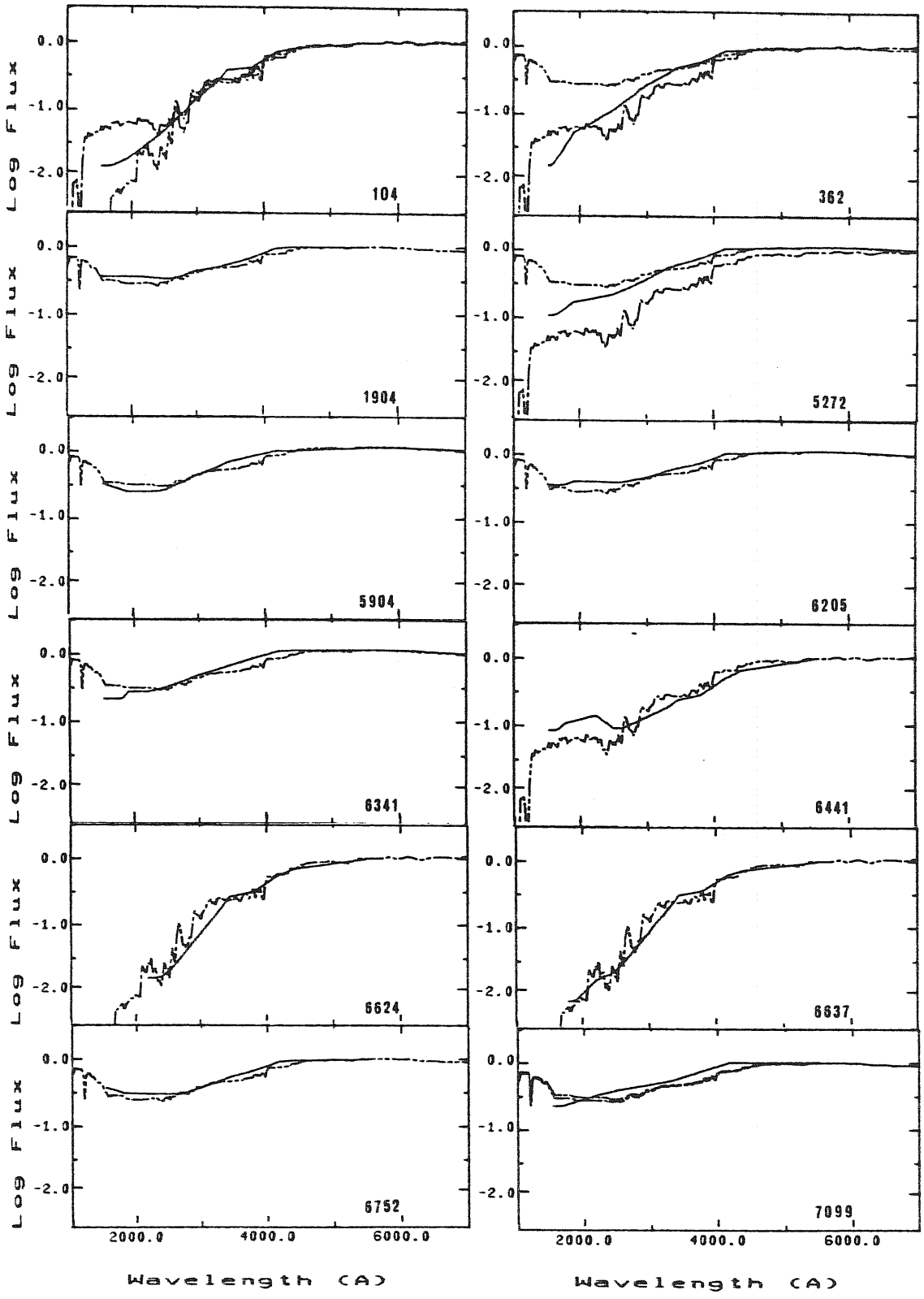

Fig. 19. SED of 12 globular clusters from data of de Boer (1985) and Faber (1973) (solid line of each panel). Superimposed are models whose identification parameter are quoted in the text.

TABLE VII

CLUSTER		[Fe/H]	HB type
104	(47 Tuc)	-0.44	7
362		-1.20	5
1904	(M79)	-1.58	-
5272	(M3)	-1.57	4
5904	(M5)	-1.25	3
6093	(M80)	-1.54	-
6205	(M13)	-1.42	1
6341	(M92)	-2.12	2
6356		-0.37	7
6441		-0.24	-
6624		-0.34	-
6637	(M69)	-0.47	7
6656	(M22)	-1.69	2
6752		-1.62	1
7099	(M30)	-2.03	1

In the following we analyse in some detail the clusters and the possibility of fitting their distributions with our models. With regard to this it must be remarked that the impossibility of getting the fit in some cases can be due to the small number of the explored chemical compositions.

NGC104: there is some disagreement between the UV spectrum of Nesci and de Boer's curve. The best fit is obtained with the synthetic spectrum with $Z=10^{-2}$ and $t=(1.5 - 1.6)\times10^{10}$ yr (in this age range the UV spectrum changes very quickly due to the rapid evolution of the HB).

NGC362: Nesci's spectrum and de Boer's UV portion of the energy distribution agree fairly well. The whole distribution curve is intermediate between the two synthetic spectra respectively with $Z=10^{-4}$ and $t=1.6\times10^{10}$ yr and $Z=10^{-2}$ and $t=1.6\times10^{10}$ yr. Since Harris and Racine (1979) give [Fe/H]=-1.20, it seems that the best fit could be obtained with a model with an intermediate metal abundance.

NGC1904 (and NGC6656): the fit with the model $Z=10^{-4}$ and

$t=1.5x10^{10}$ yr is very good.

NGC5272: this cluster has a spectrum which is intermediate between those with $Z=10^{-4}$ $t=1.6x10^{10}$ yr and $Z=10^{-2}$ and $t=1.6x10^{10}$ yr.

NGC5904 (and NGC6093): in the UV the curves derived from de Boer (1985) are in agreement with the corresponding spectra of Nesci. On the whole wavelength range in both cases the spectral distribution is fitted by the model with $Z=10^{-4}$ and $t=1.6x10^{10}$ yr, although the metal abundance, according to Harris and Racine (1979), is intermediate.

NGC6205: the observed spectrum gives a good fit with the synthetic curve with $Z=10^{-4}$ and $t=1.6x10^{10}$ yr. However in this case also the metal abundance, derived from Harris and Racine, is not so extreme.

NGC6341: the two observed sets of data (de Boer and Nesci) agree in their common portion. de Boer's curve is fitted by the model with $Z=10^{-4}$ and $t=1.6x10^{10}$ yr although some disagreement is found in the far UV and in the interval (3000 - 4500A).

NGC6441: the fit with the curve $Z=10^{-2}$ and $t=1.6x10^{10}$ yr is rather uncertain. Probably this could depend on the bad quality of the UV data.

NGC6624: de Boer's curve is fitted by the model with $Z=10^{-2}$ and $t=1.5x10^{10}$ yr. Nesci's spectrum, compared with this model, has a larger monochromatic flux for $\lambda<2000$ A. Perhaps a better fit in this case can be obtained by increasing to $1.55x10^{10}$ yr the age of the model.

NGC6637: the SED of this cluster is similar to that of NGC

6356 which shares also the same metal abundance and the same HB type. The fit is obtained with the model $Z=10^{-2}$ and $t=1.5x10^{10}$ yr.

NGC6752: its energy distribution is fitted by the model $Z=10^{-4}$ and $t=1.6x10^{10}$ yr.

NGC7099: as Harris and Racine (1979) give a very low metal content, the fit should be reached with $Z=10^{-4}$ but neither the model with $t=1.6x10^{10}$ yr nor the model with $t=1.5x10^{10}$ yr give a good result.

As has already been mentioned, the models for the group of globular clusters have been derived by supposing that the only parameter is the metal content: metal-poor clusters display a blue HB while metal-rich ones have red HBs: however the necessity of a second parameter, whose nature is still uncertain, has been stressed by several authors. If the globular clusters constitute a bi-parametric family one expects that there are clusters which can be interpreted in terms of the present calibrations and others which cannot be interpreted.

However the difference between SEDs of normal and anomalous clusters for the same type of HB is not relevant, at least if one neglects the consideration of the spectral features. This is the case, for instance, of the couples of clusters: NGC6205, NGC7099 and NGC6341, NGC6656. Both members of each couple have the same type of HB and different metal content (cf. Table VII) their SEDs are not much different. It is interesting also to compare clusters with the same metal content. Clusters NGC6752 and NGC5272 have approximately $[Fe/H]\simeq-1.6$: the former however has,

according to Dickens (1972), a type 1 HB, while the latter a type 4. The comparison of the two spectra (Fig. 20a) shows that UV fluxes are very different, the lower flux corresponding to the redder HB.

The same situation is offered also by NGC6205 and NGC362 which have [Fe/H]≈-1.4 and whose HBs are respectively of type 1 and 5 (Fig. 20b). Provided that the estimates of [Fe/H] are sufficiently correct these cases represent a confirmation of the existence of a second parameter.

8. SPECTRAL EVOLUTION OF GALAXIES.

8.1 Galactic synthetic spectral energy distributions.

Galaxy models have been derived under the following assumptions:

- the stellar birth rate is a decreasing exponential function of time: $B(t) = A\, e^{-\beta t}$ with a time scale $\tau=1/\beta$ where β has been varied in the interval (0,10), the time being measured in tens of billion years.
- the initial mass function is the Salpeter function with $\alpha=2.35$ and the calibrations of the stellar generations adopted are those described in the previous sections.
- the age of the galaxies is 1.6×10^{10} yr.
- Account is taken, although in an approximate way, of the chemical evolution of the interstellar medium. The evolution of the metal abundance is schematized by means of a one-step

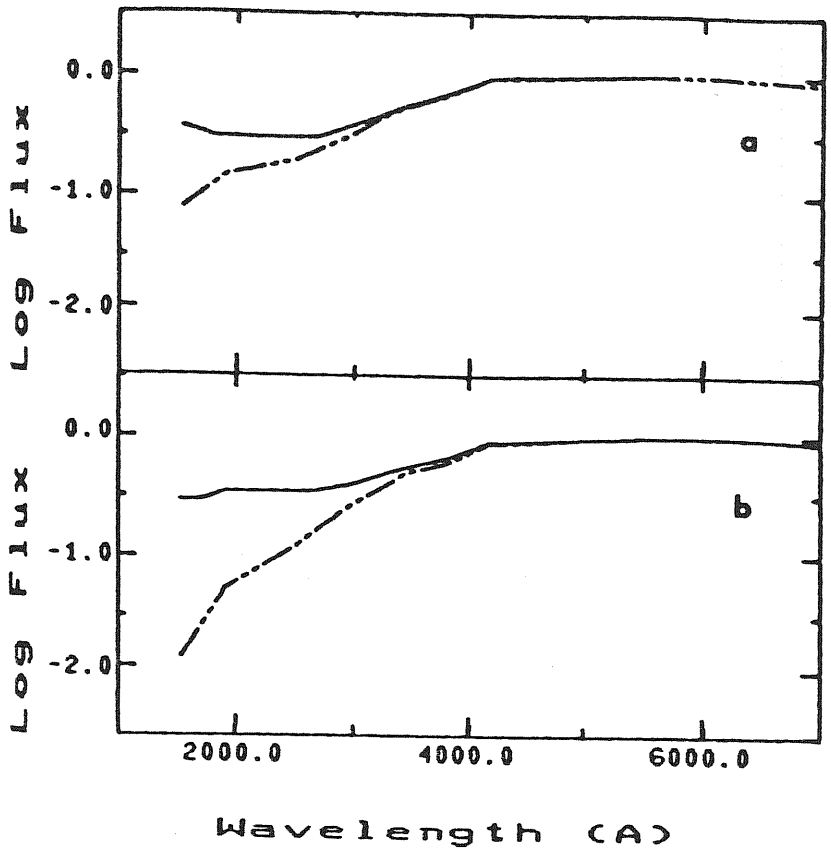

Fig. 20. a) SED of NGC6752 (upper curve) and NGC5272; b) SED of NGC6205 (upper curve) and NGC362.

function:

$$Z = 10^{-4} \qquad t < t^*$$
$$Z = 10^{-2} \qquad t > t^*$$

this rough approximation of the function Z(t) which can be derived from the simple model of Talbot and Arnett (1971), is required because only the calibrations with $Z=10^{-4}$ and $Z=10^{-2}$ are available. On the other hand, since the simple model for the chemical evolution of a closed system is also rather inaccurate, t^* should be treated as a parameter.

Fig. 21 shows some synthetic spectra computed neglecting the metal-poor population ($t^* = 0$) and for different values of the star formation timescale corresponding to β=0, 2, 5, 10. The spectral distributions are normalized at λ = 7000 A.

Each curve can be schematically interpreted as the superposition of two fundamental spectra whose relative importance depends on the value of β: the former corresponds to a very young generation (and as already remarked, is very similar to the spectrum of an early type star) the latter to an old generation. When the star formation rate is constant ($\beta = 0$) the spectrum of the young generations dominates and the resulting spectral distribution is characterized by a large UV flux. As β increases the decreasing star formation rate depresses the relative contribution of the young generations and the far UV flux becomes negligible. It must be remarked however that the models ignore the metal-poor generations which, for advanced ages, can contribute to the UV flux with their hot HB stars and moreover p-AGB stars have also been neglected. Fig. 22

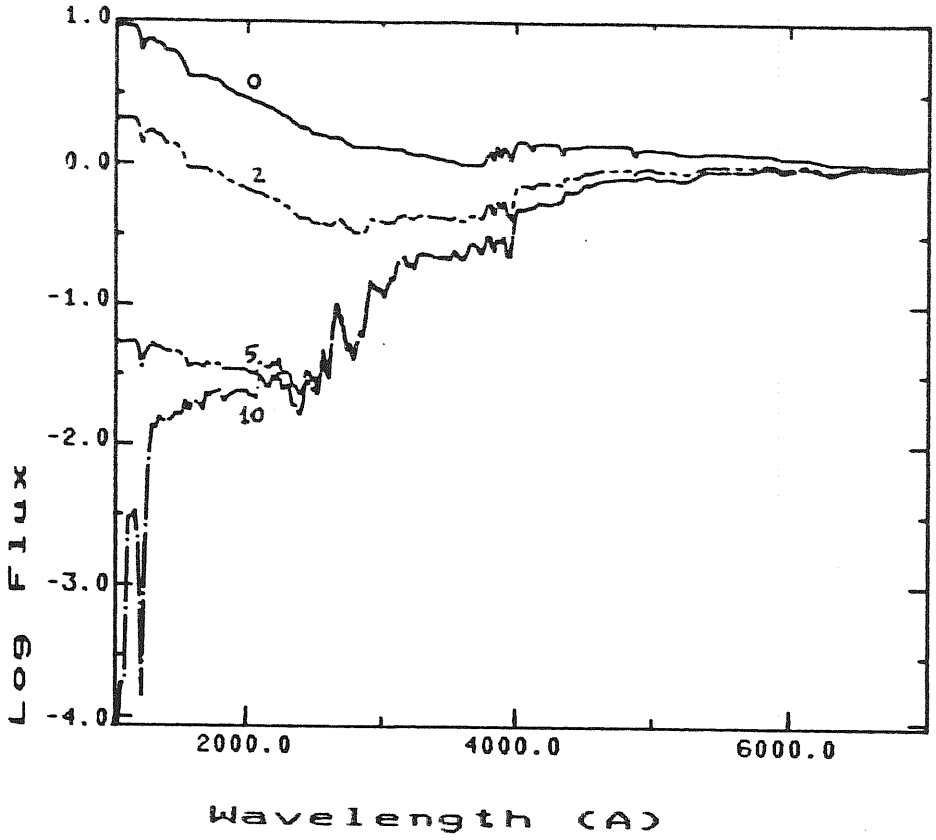

Fig. 21. Galaxy models with $t=1.6\times10^{10}$, $t^*=0$. Figures give the value of β.

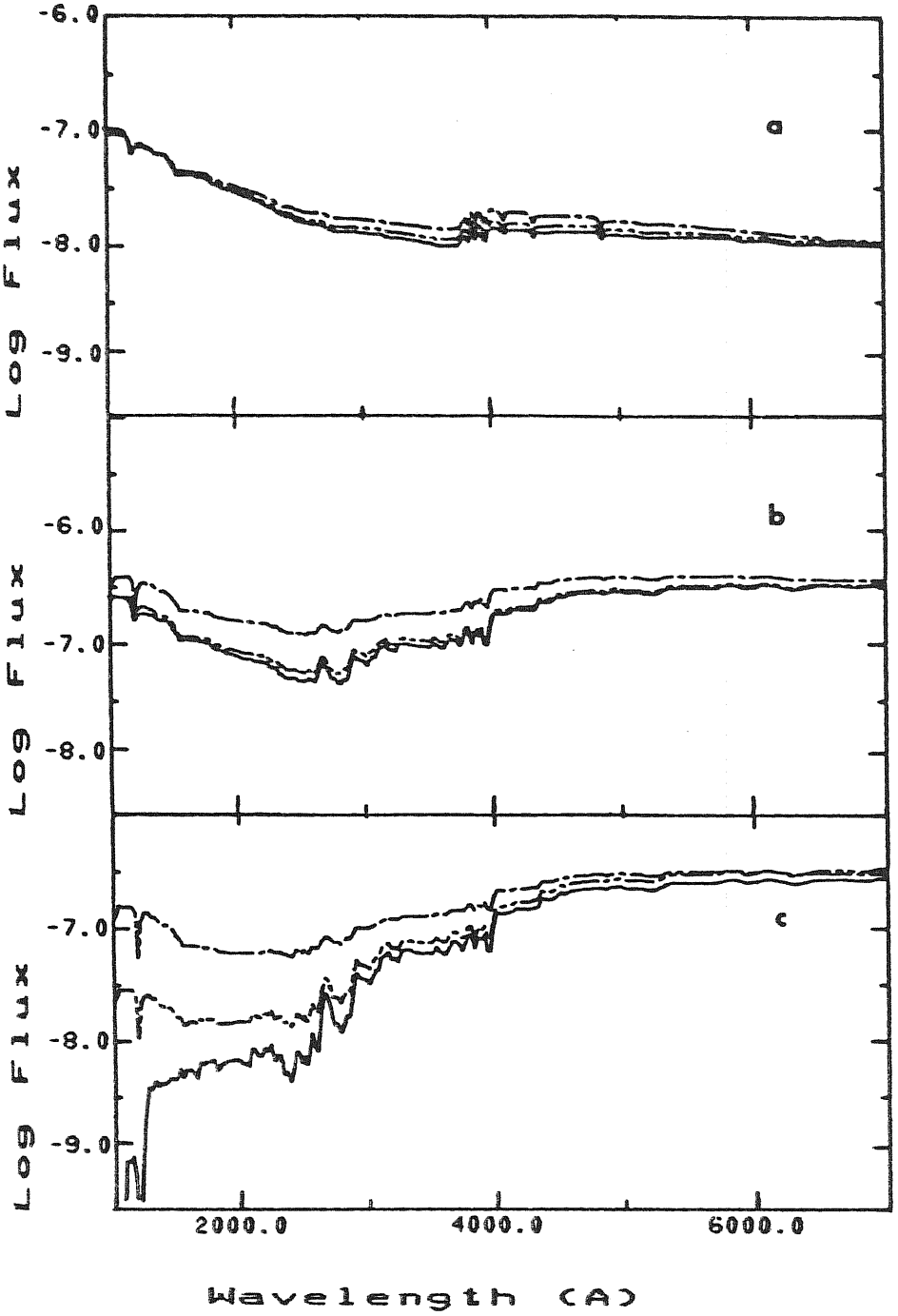

Fig. 22. Galaxy models. From top to bottom within each panel: a) β=0 t*=0, 8, 14; b) β=3 t*=0, 0.4, 4; c) β=10 t*=0, 0.12, 1 (t* in 10^9).

shows how the spectra are modified when the metal-poor population is included contributing to the total flux with a fraction which depends on the parameter t*. Obviously the inclusion of the metal-poor generations does not sensibly modify the spectrum when β is small and the galaxy spectrum is dominated by the light of the young massive stars; as β increases, however, this population affects mostly the UV region. Although the amount of the correction due to the metal-poor population depends on the value of t*, for large values of β, the inclusion of Pop. II blue HB stars can markedly affect the far UV flux. We can speculate how the modification of the exponent of the IMF from 2.35 to 3 can alter the previous results. A steeper IMF, by decreasing the number of massive stars, produces the same effect that is obtained by raising the value of β. At first sight it seems therefore impossible to distinguish between the effects of α and β on the SED; however in the far UV the maximum which appears in the spectra of young generations is strongly dependent on the slope of the continuum in this spectral region: a useful parameter for this correlation could be the ratio of the maximum flux to the minimum flux both in the UV region.

The comparison of the synthetic spectra with the observed ones is rather difficult owing to the lack of observations in the UV: in fact while UV observations of early type galaxies are relatively abundant, the same type of observations for late type galaxies is scarce since these objects, due to their low surface brightness, cannot be easily

observed with the present instruments.

The most useful data are:

- standard SEDs for the different types of galaxies, obtained by collecting observations of several authors: they represent average distributions for a given morphological type and are usually derived with the purpose of determining the K-correction. Distributions of this type have been published by Pence (1976) and by Coleman et al. (1980). The UV spectral distributions of Pence are based on the wide band photometric system of the OAO-2 satellite.
- IUE measures of the UV spectrum of single elliptical galaxies (Bertola et al. 1980, Oke et al. 1981, Bertola et al. 1982): these data are particularly interesting since they have revealed that there is an increase of monochromatic flux shortwards below λ = 2000 A.

At present we restrict ourselves to compare our models with the standard curves of Pence.

Fig. 23 shows Pence's curves for the different types on which some models are overimposed. The figures on the diagrams refer to the parameters of models. The following conclusions arise: the models which neglect the metal-poor population (t* = 0) are not able to fit the observed curves (see for instance Fig. 23a for Im - Sdm galaxies); a better agreement is obtained with models which account for the presence of this population. However in this case also some disagreement remains since in the far UV Pence's curves are steeper than the models. Provided that the observed curves are correct, such disagreement can be removed if

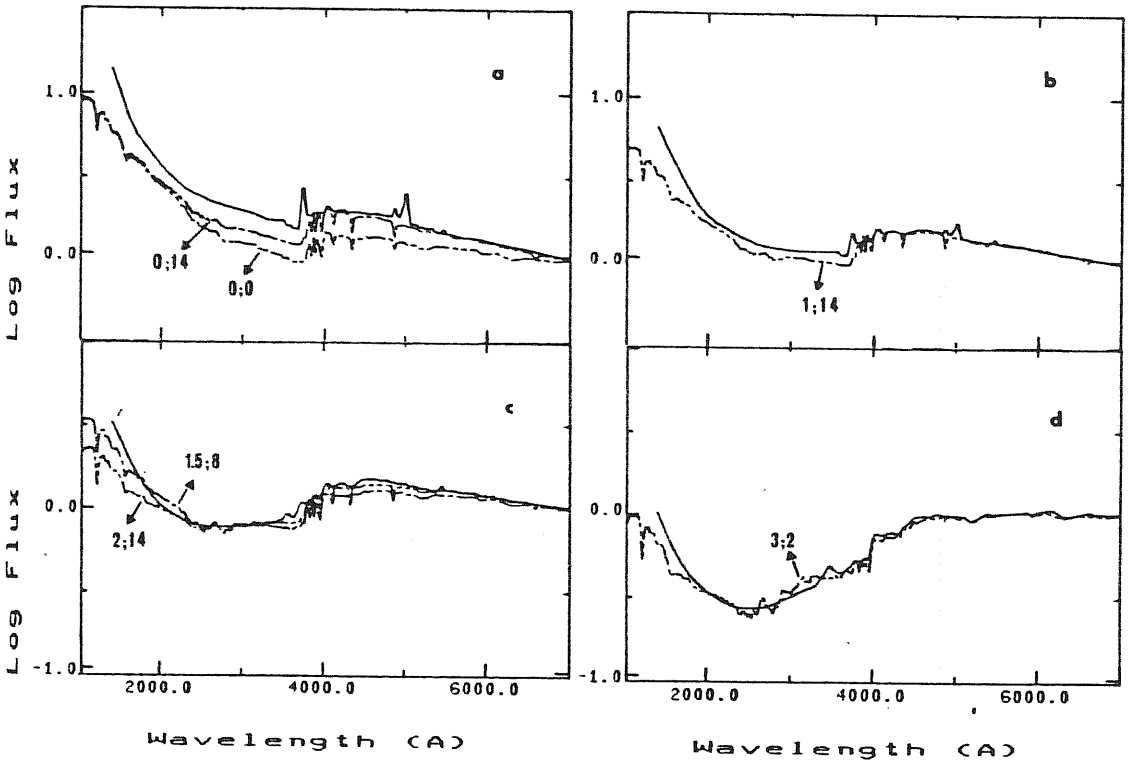

Fig. 23. Comparison of Pence's curves (solid line) with the models: a) Im-Sdm; b) Scd; c) Sbc d) Sab. The quoted numbers are respectively the values of β and t* in billion years.

a larger number of massive stars is included in the models: this result can be obtained either with an IMF flatter than that used (α = 2.35) or by adding a burst of star formation. With reference to Fig. 23a if we add to the model with α = 0 and t* = 14 a burst of star formation of the length of 10^6 yr and whose intensity is 10 times as large as the constant value of the birth-rate of the underlying model, the agreement with the observed curve is fairly good.

Elliptical galaxies have been the subject of exhaustive analyses in the last years (cf. Wu et al. 1980, Bertola 1986, Nesci 1986); the conclusion was that, at present, it is impossible to single out univocally a model able to reproduce the optical and UV spectrum. Models with a suitable percentage of hot stars can explain the upturn of the monochromatic flux in the far UV; the nature of such hot stars cannot however be determined in an unique way: in fact it has been suggested that they are young massive stars resulting from a burst of star formation, or blue Pop. II HB stars or active white dwarfs (Nesci and Perola, 1983), or nuclei of planetary nebulae, O and B subdwarfs, etc.

We only want to add a further model which accounts for both Pop. II HB stars and p-AGB stars. The model is characterized by the following parameters: age of 1.6×10^{10} yr, β = 10, α = 2.35, t* = 1.2×10^8. Furthermore, according to the prescription of Renzini and Buzzoni (1983), it has been assumed that all the generations older than 1×10^{10} yr do have p-AGB stars and their contribution to the bolometric light is 10% of the total luminosity of each generation. The mean temperature adopted for

such stars is 20000°K. The model is shown in Fig. 24, with the spectrum of NGC4649 (Bertola et al., 1982); from the comparison it turns out that the upturn in the far UV is reproduced fairly well; there is yet a discrepancy in the interval 2500-4000 A. It must be remarked, however, that Pence's standard curve for ellipticals, which is also shown in Fig. 24, fits the model at these wavelengths.

8.2 Galaxy synthetic spectral evolution.

Preliminary models of SED evolution of galaxies have been computed and presented in fig. 25.

Fig. 25a shows the evolution of a model with $\beta=0$ $t^*=3x10^9$ yr the three curves correspond to age of t_9 = 5, 10 and 16. This model is representative of Sdm - Im galaxy; it can be noted that the evolution affects mainly the red part of the SED. The UV spectrum remain essentially unchanged because it depends only on the recently formed generations which have always the same number of stars, the SFR being constant ($\beta=0$); the red flux increases with the age because it depends upon the old generations whose relative weight grows continuously.

Fig. 25b shows the evolution of a model with $\beta=3$, $t^*=5x10^9$ yr; the curves correspond to $t_9=7$, 10, 16. This model is representative of a Sab type galaxy. The total luminosity decreases, the UV preserves its shape and the red part of the SED changes its slope: initially it decreases as λ increases, afterwards it increases.

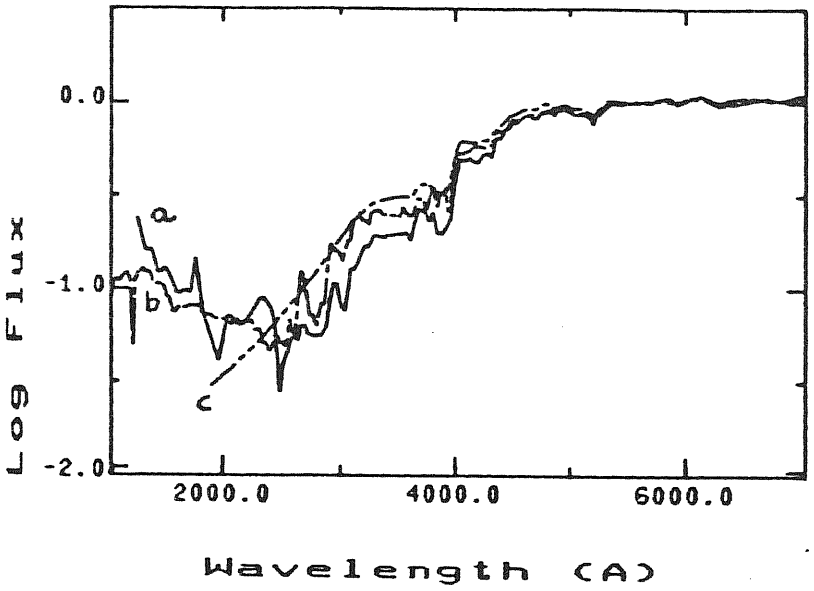

Fig. 24. Comparison of the spectra of NGC4649 (curve a) with the model including the contribution of the post-AGB (curve b). Pence's curve for ellipticals is also displayed (curve c).

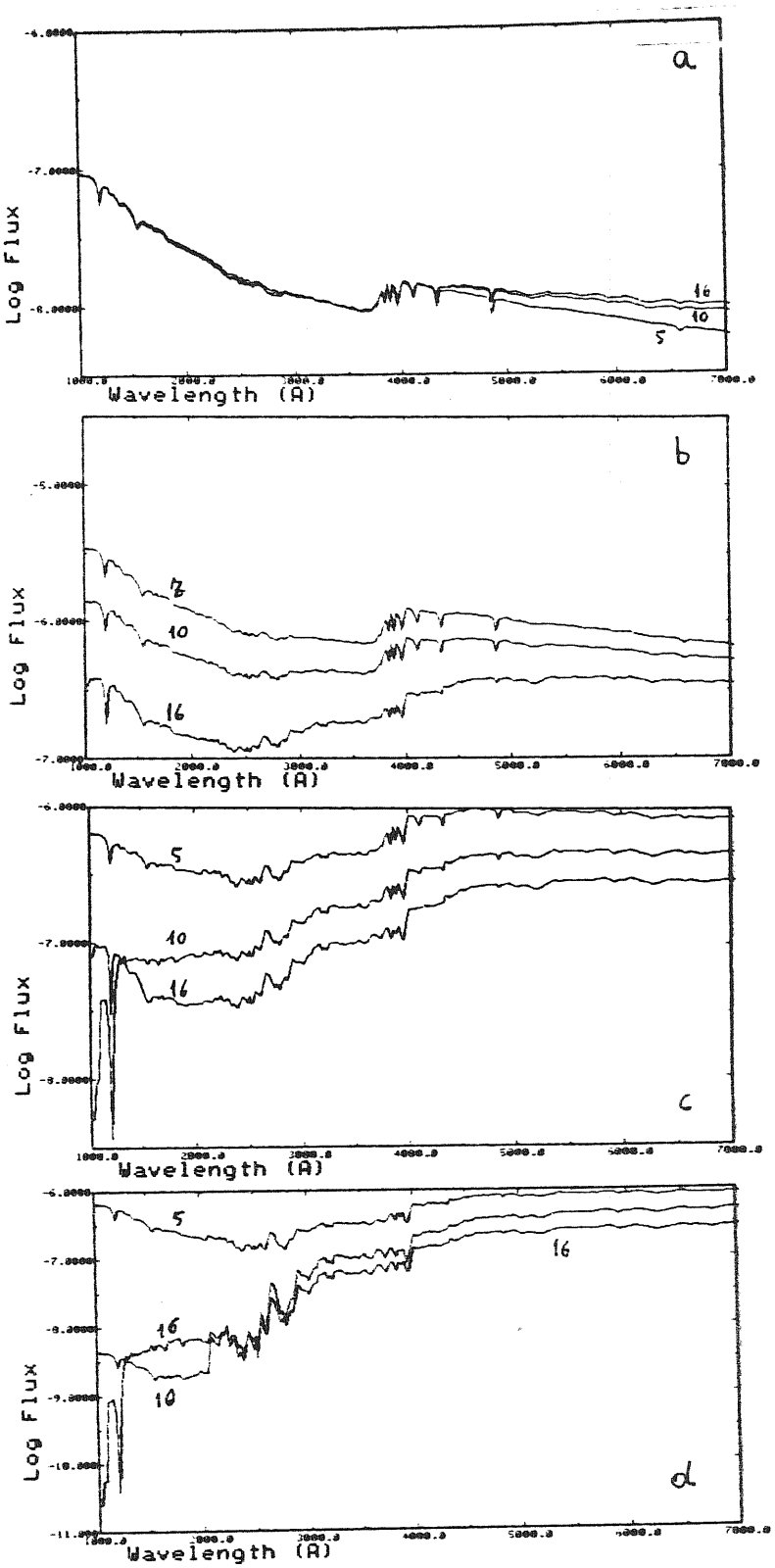

Fig. 25. Spectral evolution of galaxy models: a) β=0 and t*=8x10^9 yr; b) β=3 t*=5x10^8 yr; c) β=10 t*=5x10^8 yr; d) β=10 t*=0 yr. The quoted numbers are the ages in billion years.

In Fig. 25c and 25d the evolution of the models with β=10 at age t_9=5, 10, 16 is shown; the parameter t* has two values: respectively $5x10^8$ and 0 yr. In Fig. 25c the effect on the UV flux from the HB stars of the old metal-poor generations is evident.

8.3 Observational test for galaxy evolution.

Since long ago it has been realized that evidence of the evolution of galaxies lies within reach of our large telescopes, yet after 50 years we have still little conclusive evidence of galaxy evolution.

There are three methods by which the evolution can be tested form observations: broad-band counts of galaxies, broad-band photometric comparisons and spectrophotometric comparisons. All of these techniques, to some extent, rely upon the assumption of the homogeneity of the sample.

8.3.1 Broad-band galaxy counts.

It is expected that any significant change in the intrinsic luminosity of galaxies reveal itself as an alteration in the slope of the N_m - m relation. If galaxies were brighter in the past than they are now, then more galaxies would be counted in a given magnitude interval and hence yield a steeper slope.

The more known galaxy count surveys (Kron 1978, Koo 1981, Tyson and Jarvis 1979, Shanks et al. 1984, Hall and Mackay 1984), have shown that counts of galaxies to faint limits are entirely

consistent with the no evolution case.

The claims for evolution in the past have usually vanished when a proper analysis for both the technique and interpretation have been conducted.

8.3.2 Broad band photometric comparisons.

This technique consists of obtaining multicolor broad band photometry of a presumed homogeneous sample of galaxies and comparing the observed colours of galaxies at the high redshift end and those which are predicted by the use of the K-corrections applied to the low redshift sample. If there are any deviations, then one explanation might be that the discrepancy is due to something other than the redshift e. g. spectral evolution.

In general evolution is not evident, only the photometry of the first ranked clusters was shown to deviate significantly from the predicted relation (Gunn 1982). This technique can still yield useful results if enough faint rich clusters can be located; with current photographic technology, clusters with redshifts between 0.8 ÷ 1.0 can be straightforwardly discovered.

8.3.3 Spectrophotometric comparisons.

A much more straightforward technique than those outlined above, is to obtain good signal to noise ratio spectrophotometry of a homogeneous sample. This technique has several advantage in that: 1) a redshift is obtained, 2) monochromatic magnitudes can

be defined and therefore the need for K-corrections can be avoided altogether and 3) accurate indices and line-strength can be derived. The principal disadvantages at the technique is that only a limited number of objects can be observed.

Before any observational program is begun, it is imperative that the potential biases be evaluated: selection effects afflict nearly every observational program in cosmology. The traditional selection criteria is rich-cluster morphology or the strength of the radio flux density, recently a new criterion has been introduced according to the optical colours of galaxies.

The survey of the first ranked cluster galaxies are extended as far as z = 0.8 (Oke 1971, Wilkinson and Oke 1978 and Oke 1984). They have not found significantly change.

In recent years observational studies of galaxies selected by their radio flux density have been very popular (e.g. Lilly and Longair 1982, Lilly et al. 1984). The problems associated with the use of radio galaxies in cosmological studies are very large: it has been noted (van den Bergh 1975) that burst of star formation and the existence of a radio source are correlate, and it is not possible to uniquely model the evolutionary behaviour of galaxies with random or episodic star formation with the constraints of present epoch observations.

Redshifts for 3CR galaxies up to z=1.8 have been readily measured, it is clear that there is an abrupt change in the morphology at about z=1, at which changes in the spectral properties also correspond. But because of the large number of problems associated with the use of radio galaxies any far

reaching conclusions based on such data should be treated with circumspection.

New surveys of selected galaxies according to their redness relative to the typical galaxy at the same brightness level, shows that spectral evolution is less than 7% at the very highest redshift galaxies surveyed ($z \approx 0.8$) (Hamilton 1985).

Concluding, the evidence for spectral evolution in recent years has not be solid. Many of the claims for detection have vanished when a proper analysis of both the interpretations and of the techniques involved have been conducted.

REFERENCES.

Auer, L.H., Mihalas, D., 1972, Astrophys. J. Suppl. 24, 193.

Barbaro, G., Pigatto, L., 1984, Astron. Astrophys. 136, 281.

Bertelli, G., Bressan, A., Chiosi, C., 1984, Astron. Astrophys. 130, 279.

Bertelli, G., Bressan, A., Chiosi, C., 1985, Astron. Astrophys. 150, 33.

Bertelli, G., Bressan, A., Chiosi, C., Angerer, K., 1986, Astron. Astrophys. Suppl., in press.

Bertola, F., 1986, Spectral Evolution of Galaxies, eds. C. Chiosi and A. Renzini, p. 363, Dordrecht: Reidel.

Bertola, F., Capaccioli, M., Holm, A.V., Oke, J.B., 1980, Astrophys. J. 237, L65.

Bertola, F., Capaccioli, M., Oke, J.B., 1982, Astrophys. J. 254, 494.

Becker, S.A., Iben I.Jr., 1979, Astrophys. J. 238, 831.

Bisiacchi, G.F., Firmani, C., Sarmiento, A.F., 1982, Astron. Astrophys. 119, 167.

Bohlin, R.C., Holm, A.V., Savage, B.D., Snijders, M.A.J., Sparks, W.M., 1980, Astron. Astrophys. 85, 1.

Bressan, A., Bertelli, G., Chiosi, C., 1981, Astron. Astrophys. 102, 25.

Bressan, A., Bertelli, G., Chiosi, C., 1986, preprint.

Bruzual, G., 1981, Ph D. Thesis, University of California, Berkely.

Bruzual, G., Kron, R., 1980, Astrophys. J. 241, 25.

Cannon, R.D., 1970, M.N.R.A.S. 150, 111.

Capuzzo-Dolcetta, R., Kurucz, R., Rossi, R., 1983, Mem. S.A.It. 54, 829.

Chiosi, C., 1986, Spectral Evolution of Galaxies, eds. C. Chiosi and A. Renzini, p. 237, Dordrecht: Reidel.

Ciardullo, R.B., Demarque, P., 1977, Yale Trans. 33.

Ciardullo, R.B., Demarque, P., 1979, Dudley Obs. Rpt. 14, 317.

Code, A.D., Meade, M.R., 1979, Astrophys. J. Suppl. 39, 195.

Cohen, J.G., 1982, Astrophys. J. 258, 153.

Cohen, J.G., Rich, R.M., Persson, S.E., 1984, Astrophys. J. 285, 595.

Coleman, G.D., Wu, C.C., Weedman, D.W., 1980, Astrophys. J. Suppl. 43, 393.

Davis, M., Geller, M.J., Huchra, J.P., 1979, Astrophys. J. 221, 1.

de Boer, K.S., 1985, Astron. Astrophys. 142, 321.

Dickens, R.J., 1972, M.N.R.A.S. 157, 281.

Di Fazio, A., Capuzzo-Dolcetta, R., 1986, Spectral Evolution of Galaxies, eds. C. Chiosi and A. Renzini, p. 47, Dordrecht: Reidel.

Dostal, V.A., 1979, Sov. A. J., 23, 135.

Ellis, R., 1983, The Origin and Evolution of Galaxies, eds. B.J.T. Jones and J.E. Jones, p. 255, Dordrecht: Reidel.

Faber, S.M., 1973, Astrophys. J. 179, 731.

Felten, J.E., 1977, Astron. J. 82, 861.

Fusi-Pecci, F., Renzini, A., 1975, Astron. Astrophys. 39, 413.

Garmany, C.D., Conti, P.S., Chiosi, C., 1982, Astrophys. J. 263,

777.

Gunn, J.E., 1982, Astrophysical Cosmology, eds. H.A. Bruck, G.V. Coyne, and M.S. Longair, p. 233.

Hall, P., Mackey, C., 1984, M.N.R.A.S. 210, 979.

Hamilton, D., 1985, Astrophys. J. 297, 371.

Harris, W.E., Racine, R., 1979, Ann. Rev. Astron. Astrophys. 17, 241.

Hodge, P.W., 1983, Astrophys. J. 264, 470.

Hubble, E.P., 1926, Astrophys. J. 64, 231.

Huchra, J.P., 1977, Astrophys. J. 217, 928.

Huchra, J.P., 1978, Large Scale Structure of Universe, IAU Symposium 79, eds. M. Longair and J Einasto, p. 271, Dordrecht: Reidel.

Iben I.Jr., 1977, Astrophys. J. 217, 788.

Iben I.Jr., 1981, Astrophys. J. 246, 278.

Iben I.Jr., Renzini A., 1983, Ann. Rev. Astron. Astrophys. 21, 271.

Jamar, C., Macau-Hercot, D., Monfils, A., Thompson, G., Houziaux, L., Wilson, R., 1976, Ultraviolet Bright Stars Spectrophotometric Catalogue, ESA SR-27.

Kirschner, R.P., Oemler, A., Schecter, P.L., 1979, Astron. J. 84, 951.

Kristian, J., Sandage, A., Westphal, J.A., 1978, Astrophys. J. 221, 383.

Koo, D., 1981, Ph. D. Thesis, University of California Berkeley.

Kron, G., 1978, Ph. D. Thesis, University of California, Berkeley.

Kurucz, R., 1979, Astrophys. J. Suppl. 40, 1.

Lattanzio, J.C., 1986, preprint.

Larson, R.B., 1986, M.N.R.A.S. 218, 409.

Larson, R.B., Tinsley B.M., 1974, Astrophys. J. 192, 1.

Lequeux, J., 1979, Astron. Astrophys. 80, 35.

Lilly, S., Longair, M.S., 1982, M.N.R.A.S. 199, 1053.

Lilly, S., McClean, I., Longair, M.S., 1984, M.N.R.A.S. 209, 401.

Macau-Hercot, D., Jamar, C., Monfils, A., Thompson, G., Houziaux, L., Wilson, R., 1978, Suppl. to the Ultraviolet Bright Stars Spectrophotometric Catalogue, ESA SR-28.

Malagnini, M.L., Faraggiana, R., Morossi, C., 1983, Astron. Astrophys. 128, 375.

Malagnini, M.L., Faraggiana, R., Morossi, C., Crivellari, L., 1982, Astron. Astrophys. 114, 170.

Matteucci, F., Tornambe', A., 1985, Astron. Astrophys. 142, 13.

Meade, M.R., Code, A.D., 1980, Astrophys. J. Suppl. 42, 283.

Miller, G.E., Scalo, J.M., 1979, Astrophys. J. Suppl. 41, 513.

Nesci, R., 1981, Astron. Astrophys. 99, 120.

Nesci, R., 1986, Spectral Evolution of Galaxies, eds. C. Chiosi and A. Renzini, p. 369, Dordrecht: Reidel.

Nesci, R., Perola, G.C., 1983, Mem. S.A.It. 54, 851.

Nomoto, K., 1984, in Stellar Nucleosynthesis, eds. C. Chiosi and A. Renzini, p. 239, Dordrecht: Reidel.

Oke, J.B., 1971, Astrophys. J. 170, 193.

Oke, J.B., 1984, Clusters and Groups of Galaxies, eds. F. Mardirossian, G. Giuricin, and M. Mezetti, p. 99, Dordrecht: Reidel.

Oke, J.B., Bertola, F., Capaccioli, M., 1981, Astrophys. J. 243, 453.

Paczynski, B., 1971, Acta Astron. 21, 271.

Pence, W., 1976, Astrophys. J. 203, 39.

Rana, N.C., Wilkinson, D.A., 1986, M.N.R.A.S., 218, 497.

Reimers, D., 1975, Proceed. of 19 Colloque International d'Astrophysique, Liege, 369.

Remie, H., Lamers, H.J.G.L.M., 1982, Astron. Astrophys. 105, 20.

Renzini, A., Buzzoni, A., 1983, Mem. S.A.It. 54, 739.

Renzini, A., Voli, M., 1981, Astron. Astrophys. 94, 175.

Rood, R.T., 1973, Astrophys. J. 184, 815.

Salpeter, E.E., 1955, Astrophys. J. 121, 61.

Sandage, A., 1961, Astrophys. J. 133, 355.

Searle, L., Wilkinson, A., Bagnuolo, W.G., 1973, Astrophys. J. 239, 803.

Seaton, M.S., 1979, M.N.R.A.S. 187, 738.

Schecter, P.L., 1976, Astrophys. J., 203, 297.

Schmidt, M., 1959, Astrophys. J. 129, 243.

Shanks, T., Stevenson, P., Fong, R., 1984, M.N.R.A.S. 206, 767.

Straizys, V., Sviderskiene, Z., 1972, Bull. Vilnius Astron. Obs. 35, 1.

Sweigart, A.V., Gross, P.G., 1976, Astrophys. J. Suppl. 32, 367.

Talbot, R.J., 1980, Astrophys. J. 235, 821.

Talbot, R.J., Arnett, W.D., 1971, Astrophys. J. 170, 409.

Tamman, G.A., Yahil, A., Sandage, A., 1980, Astrophys. J. 234, 775.

Thuan, T.X., Gunn, J.E., 1976, Pub. A.S.P. 88, 543.

Tinsley, B.M., 1980, Astrophys. J. 241, 41.

Tinsley, B.M., 1981, Cosmologique Physique - Physical Cosmology, eds. R. Balian, J. Audouze and D.N. Schramm, p. 162, Amsterdam: North-Holland.

Turner, E.L., Gott, 1976, Astrophys. J. 209, 6.

Tyson, A., Jarvis, J., 1979, Astrophys. J. Lett. 230, L153.

Underhill, A.B., 1980, Astrophys. J. 239, 220.

van den Bergh, S., 1960, Publ. DDO 2, 159.

van den Bergh, S., 1975, Ann. Rev. Astron. Astrophys., 13, 217.

Wilkinson, A., Oke, J.B., 1978, Astrophys. J. 220, 237.

Wipple, F.L., 1935, Harvard College Obs. Circ. 404, 1.

Wu, C.C., Faber, S.M., Gallagher, J.S., Peck, M., Tinsley, B.M., 1980, Astrophys. J. 237, 290.